frontiers | Frontiers in Chemistry

TYPE Review
PUBLISHED 27 January 2023
DOI 10.3389/fchem.2023.1126309

OPEN ACCESS

EDITED BY
Haidong Li,
Dalian University of Technology, China

REVIEWED BY
Fabiao Yu,
Hainan Medical University, China
Jin Zhou,
Weifang Medical University, China
Xin Li,
Zhejiang University, China

*CORRESPONDENCE
Huawei Niu,
✉ niuhw0816@126.com
Shan Wang,
✉ smallcoral@live.cn

SPECIALTY SECTION
This article was submitted to Chemical Biology,
a section of the journal
Frontiers in Chemistry

RECEIVED 17 December 2022
ACCEPTED 16 January 2023
PUBLISHED 27 January 2023

CITATION
Jia T-T, Zhang Y, Hou J-T, Niu H and Wang S (2023), H_2S-based fluorescent imaging for pathophysiological processes. *Front. Chem.* 11:1126309.
doi: 10.3389/fchem.2023.1126309

H_2S-based fluorescent imaging for pathophysiological processes

Tong-Tong Jia[1], Yuanyuan Zhang[2], Ji-Ting Hou[3], Huawei Niu[2]* and Shan Wang[4]*

[1]College of Chemistry and Chemical Engineering, Luoyang Normal University, Luoyang, China, [2]College of Food and Bioengineering, Henan University of Science and Technology, Luoyang, China, [3]National Engineering Research Center of Ophthalmology and Optometry, Eye Hospital, Wenzhou Medical University, Wenzhou, China, [4]Key Laboratory of Intelligent Treatment and Life Support for Critical Diseases of Zhejiang Province, The First Affiliated Hospital of Wenzhou Medical University, Wenzhou, China

Hydrogen sulfide (H_2S), as an important endogenous signaling molecule, plays a vital role in many physiological processes. The abnormal behaviors of hydrogen sulfide in organisms may lead to various pathophysiological processes. Monitoring the changes in hydrogen sulfide is helpful for pre-warning and treating these pathophysiological processes. Fluorescence imaging techniques can be used to observe changes in the concentration of analytes in organisms in real-time. Therefore, employing fluorescent probes imaging to investigate the behaviors of hydrogen sulfide in pathophysiological processes is vital. This paper reviews the design strategy and sensing mechanisms of hydrogen sulfide-based fluorescent probes, focusing on imaging applications in various pathophysiological processes, including neurodegenerative diseases, inflammation, apoptosis, oxidative stress, organ injury, and diabetes. This review not only demonstrates the specific value of hydrogen sulfide fluorescent probes in preclinical studies but also illuminates the potential application in clinical diagnostics.

KEYWORDS

fluorescence probe, hydrogen sulfide, pathophysiological processes, biomarker, visualization

1 Introduction

Hydrogen sulfide (H_2S) is the third gaseous signaling molecule found after carbon monoxide (CO) and nitric oxide (NO) (Szabo et al., 2013). Unlike other signaling molecules, H_2S can freely penetrate the cell membrane without affecting the cell's signaling response (Predmore et al., 2012). H_2S is present both inside and outside the cell and is widely recognized in regulating nervous systems, cellular bioenergetics and metabolism, gene transcription and translation, vascular tone, and immune function (Cirino et al., 2022). Endogenous H_2S is principally produced by three kinds of biological enzymes, including cystathionine γ-lyase (CSE), cystathionine β-synthase (CBS), and 3-mercaptopyruvate sulfurtransferase (3-MST) (Szabo et al., 2013; Augsburger and Szabo, 2020; Zhang et al., 2021). The physiological concentration of H_2S ranges from 0.01 to 3 μM at the cellular level and 30–100 μM in serum (Wallace, 2007). H_2S plays an indispensable role in physiological processes, for example, angiogenesis, neurotransmission, apoptosis, and insulin secretion (Austgen et al., 2011; Papapetropoulos, 2016; Bełtowski et al., 2018; Wang et al., 2020). Furthermore, aberrant H_2S levels are strongly related to various pathophysiological processes, such as neurodegenerative diseases, liver cirrhosis, inflammation, and cancer (Kamoun et al., 2003; Chan and Wong, 2017; Wei et al., 2017; Bełtowski et al., 2018; Disbrow et al., 2021; Kushkevych et al., 2021; Ngowi et al., 2021). Hence, exploring validated assays for H_2S is essential to better understand and diagnose their pathophysiological processes.

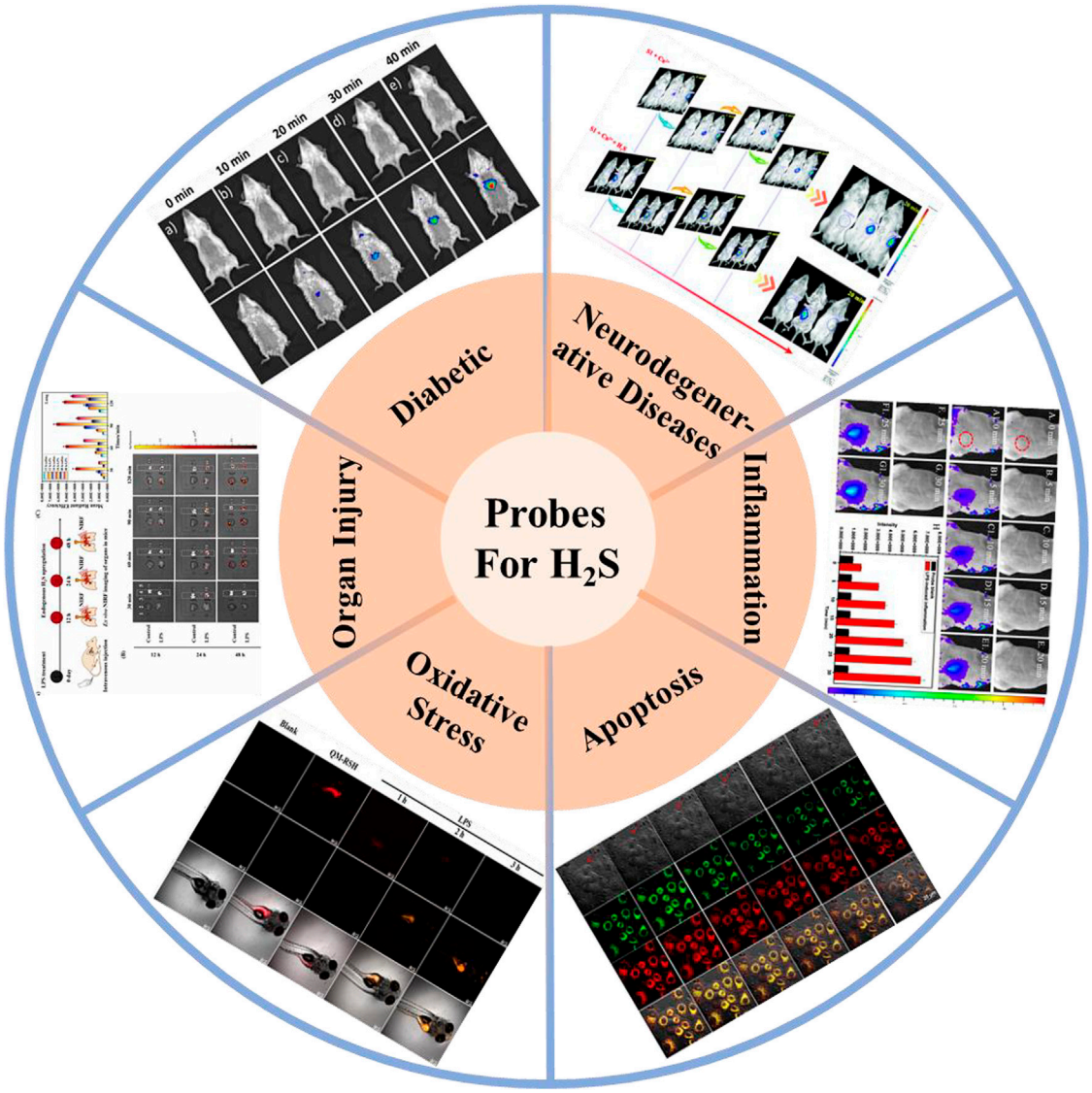

FIGURE 1
H_2S-based small organic fluorescent probes for imaging and diagnosis of pathophysiological processes.

Compared with traditional imaging methods, including magnetic resonance imaging (MRI), computed tomography (CT) and ultrasound imaging (Poelma, 2016; Lim et al., 2019; Antequera et al., 2021), fluorescence imaging technology allows non-invasive detecting biomarkers with high sensitivity, quick response time and wonderful spatiotemporal resolution, which makes animal models of tracking pathology and clinical studies very attractive (Jun et al., 2020; Hanaoka et al., 2022; Qi et al., 2022; Sun et al., 2022). Fluorescence-based imaging typically uses small molecule fluorescent probes that are designed to bind/react with disease-based target biomarkers and offer measurable fluorescent signal changes for qualitative and quantitative analysis of analytes and imaging traces (Jia et al., 2022; Zhao L et al., 2022; Hou et al., 2022; Hou et al., 2020a; Gardner et al., 2021; Du et al., 2023; Li et al., 2023). Typically, these probes should exhibit wonderful sensitivity and specificity for biomarkers to guarantee their accurate detection in bio-systems (Hou et al., 2020b; He et al., 2021; Kawai et al., 2021; Ren M et al., 2021).

This work systematically reviews the research progress of H_2S-based fluorescent probes in pathophysiological processes imaging and classifies fluorescent probes according to pathophysiological models (neurodegenerative diseases, inflammation, oxidative stress, cell apoptosis, organ injury, and diabetes), and introduces in detail the methods, means and design ideas for constructing various disease models (Figure 1). The design tactics, optical properties, response mechanism, and potential applications of these probes are discussed (Figure 2). Furthermore, we mainly focus on the biological application and significance of H_2S in pathophysiological pathological processes. Finally, we discuss the progress and insufficiencies of reported fluorescent probes for H_2S-related pathophysiological processes imaging and provide our insights on how to overcome these limitations. Hence, this paper will offer new thoughts and strategies for the development of novel fluorescent probes fitting for early warning of H_2S-related pathophysiological processes.

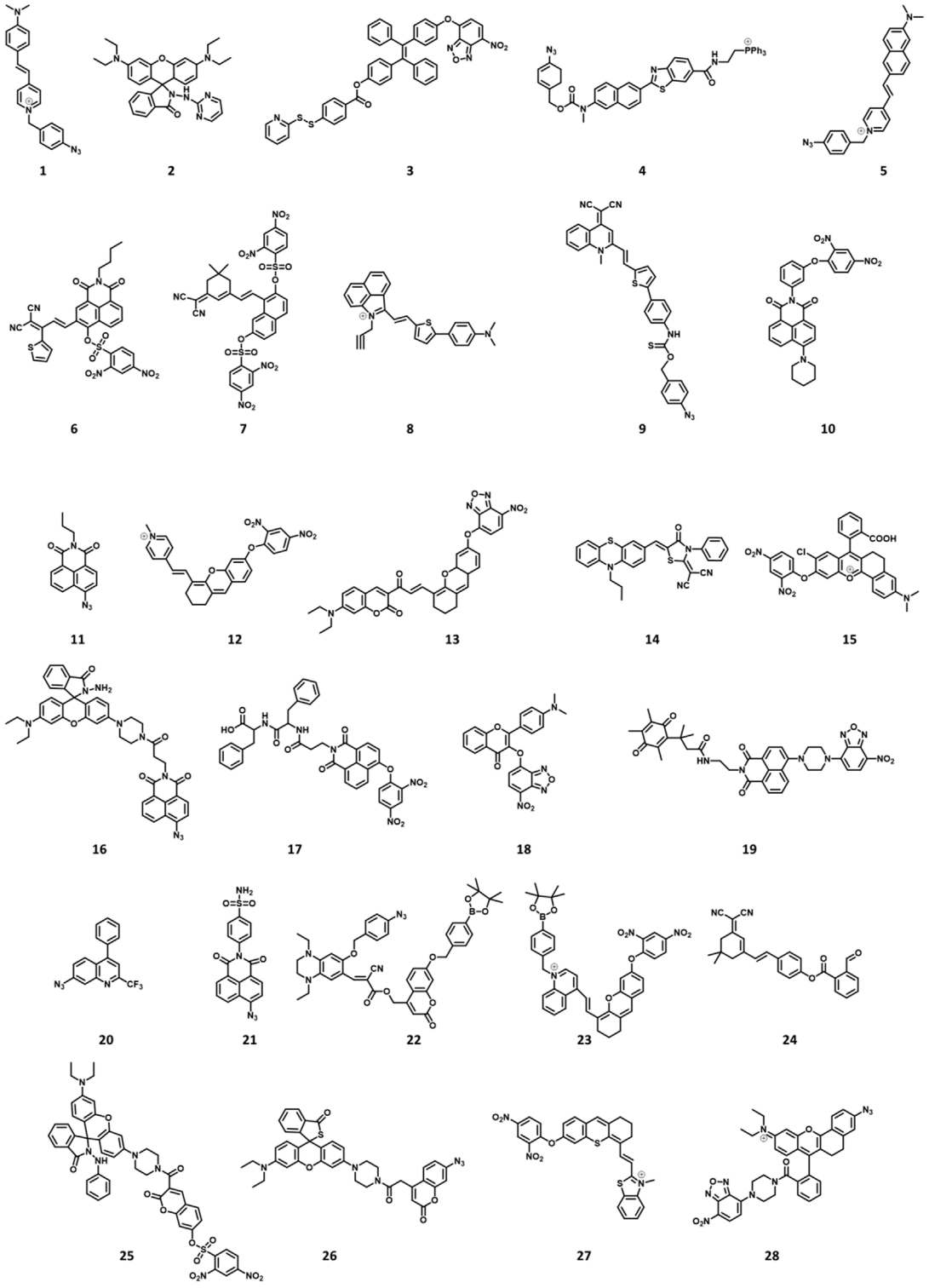

FIGURE 2
Chemical structures of H_2S-responsive probes (1, Li et al., 2018; 2, Ma et al., 2019; 3, Ramya et al., 2022; 4, Bae et al., 2013; 5, Fang et al., 2020; 6, Shen et al., 2021; 7, Kong et al., 2021; 8, Li H et al., 2022; 9, Liang et al., 2022; 10, Ou et al., 2021; 11, Ding et al., 2022; 12, Gong et al., 2021; 13, Wang K et al., 2022; 14, Hu et al., 2021; 15, Wang WX et al., 2022; 16, Ren TB et al., 2021; 17, Singh et al., 2021; 18, Liu et al., 2022; 19, Zhang et al., 2019; 20, Zhu et al., 2020a; 21, Zhu et al., 2020b; 22, Yang et al., 2020; 23, Wang Y et al., 2022; 24, Shu et al., 2020; 25, Tang et al., 2021; 26, Jiao et al., 2018; 27, Su et al., 2022; 28, Li P et al., 2022).

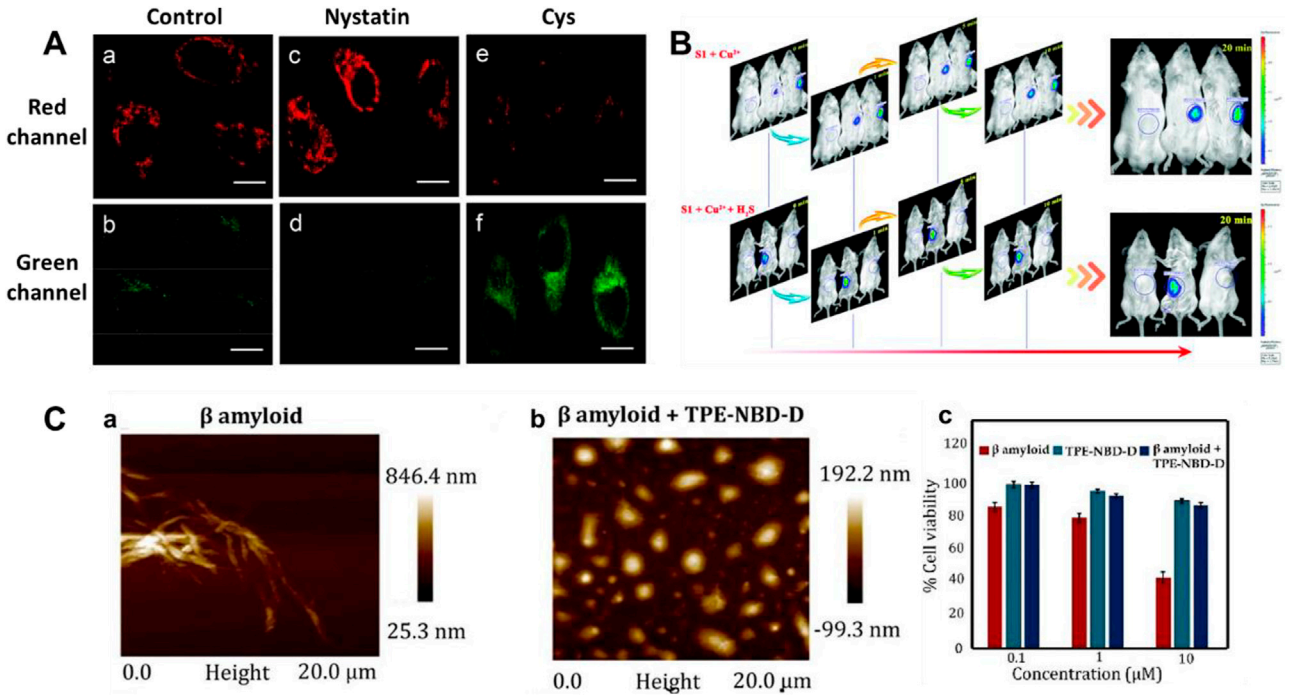

FIGURE 3
(A) Confocal imaging of the cross-talk influence of H_2S and viscosity in HeLa cells using probe 1 (reproduced from (Li et al., 2018) with permission from American Chemical Society). **(B)** Time-based *in vivo* fluorescence imaging of Cu^{2+} or Cu^{2+} + H_2S in Kunming Mice using probe 2 (reproduced from (Ma et al., 2019) with permission from the Royal Society of Chemistry). **(C)** AFM images and cytotoxicity of β sheet rich agglomerated form of $A\beta_{1-42}$ and de-agglomerated smaller $A\beta_{1-42}$ aggregates formed after incubation with probe 3 (reproduced from (Ramya et al., 2022) with permission from Elsevier (B. V).

2 Design strategy for H_2S fluorescent probes

To meet the requirements of biological applications, H_2S-based fluorescent probes for assessing pathophysiological processes-relevant should satisfy the following requirements: 1) Noteworthy signal changes after identification of H_2S, and prefer fluorescence enhancement change or ratiometric fluorescence changes to reduce background noise and maximize spatial resolution; 2) fluorophores with excellent photostability, high fluorescence quantum yield, and wonderful biocompatibility; 3) the ideal fluorescent probe should respond quickly to H_2S with wonderful selectivity and sensitivity; 4) organic solvents used as little as possible, because it will damage the function of biomolecules; 5) the identification system of the probes should be silent to biomarkers, for example, HEPES (4-(2-hydroxyethyl)piperazine-1-ethanesulfonic acid) buffers react easily with hypochlorous acid (HOCl) (Xing et al., 2016).

3 H_2S-based imaging of fluorescent probe pathophysiological processes models

3.1 Neurodegenerative diseases imaging

3.1.1 Alzheimer's disease imaging

Alzheimer's disease (AD) is an age-related neurodegenerative disorder that can lead to dementia, usually affecting people over the age of 60 (Morales et al., 2014). The aggregation of amyloid-beta (Aβ) aggregates in the central nervous system may cause and exacerbate AD, and breaking down or stopping the formation of Aβ aggregates is a vital challenge in overcoming AD (Wood, 2017; Cao L et al., 2018; Starling, 2018; Lin et al., 2019). H_2S donor, such as sodium sulfide (Na_2S), reduces the generation of Aβ, thereby providing neuroprotection against Aβ aggregates and alleviating AD (Kshirsagar et al., 2020; Tabassum et al., 2020).

Mitochondria have been used as therapeutic targets for AD (Reddy, 2009; Wang and Chen, 2016; Swerdlow, 2018). In 2018, Li et al. reported a mitochondria-targeting bifunctional fluorescent probe **1** for studying the behavior between viscosity and H_2S in mitochondria (Li et al., 2018). A significant green fluorescence enhancement was found at approximately 510 nm after the introduction of H_2S. Figure 3A showed the cross-talk influence of H_2S and viscosity in cellular mitochondria: The enlargement in viscosity may result in the reduction in H_2S, while the increase in H_2S might lead to the decrease in viscosity. This will be helpful for understanding the pathogenesis of AD.

Cu^{2+} accumulation or H_2S deficiency is closely related to AD (Cui W et al., 2016; Vandini et al., 2019). In 2019, Ma et al. reported an "OFF-ON-OFF" fluorescent probe **2** for reversible testing Cu^{2+} and H_2S. Probe **2** could be used to track Cu^{2+} and H_2S sequentially and reversibly through changes in its fluorescence signal at 580 nm. Probe **2** exhibited extremely low cytotoxicity and excellent membrane permeability. Figure 3B showed that with increasing Cu^{2+} concentration, the fluorescence in mice was significantly enhanced, while it disappeared upon the addition of H_2S. In addition, the probe had the potential ability to disassemble Cu^{2+}-induced Aβ aggregates.

Aggregation-induced emission (AIE)-based probes have wonderful features owing to their tunable emission, favorable

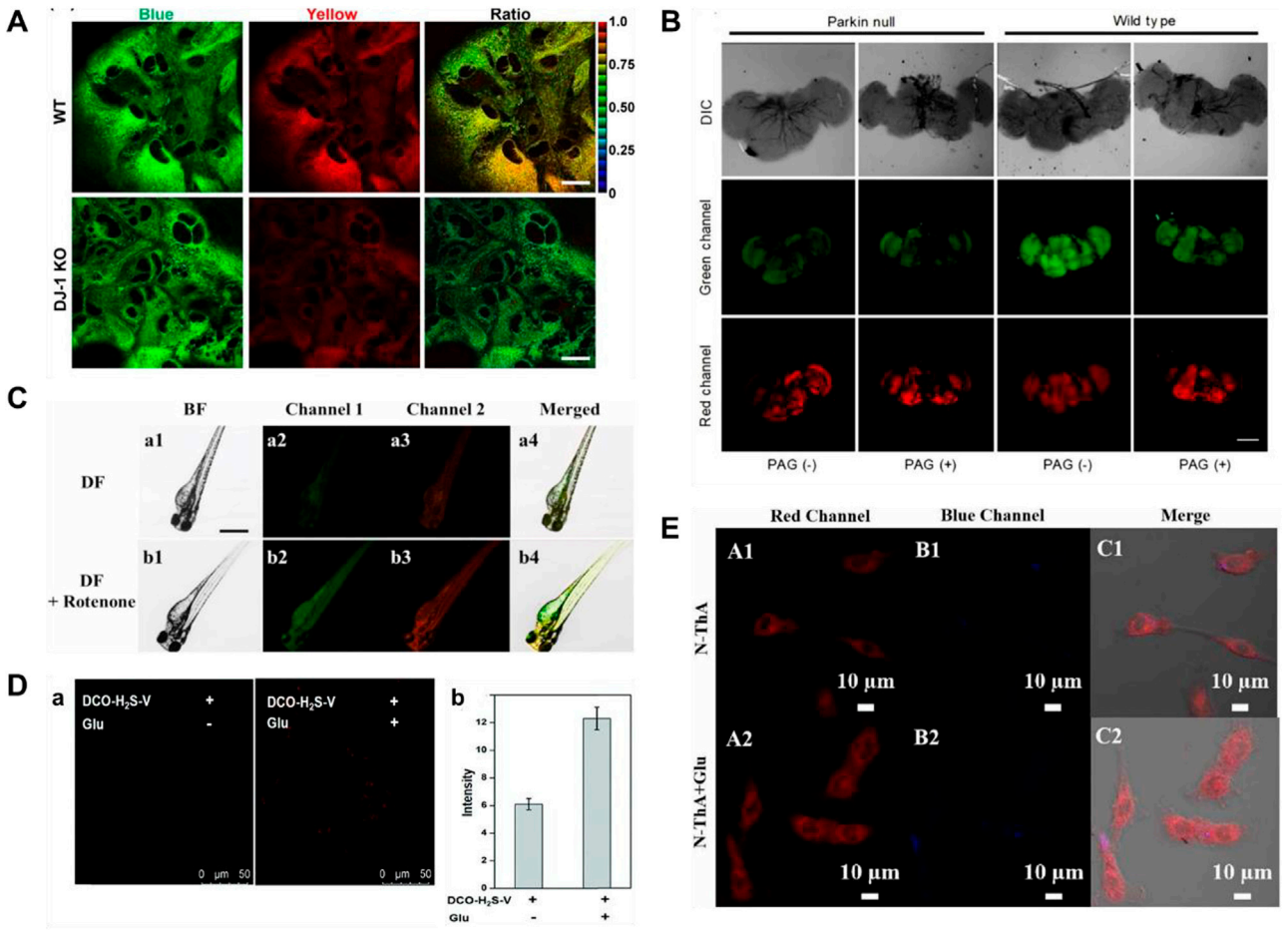

FIGURE 4
(A) Probe 4 displayed the correlation between CBS expression and H_2S levels (reproduced from (Bae et al., 2013) with permission from American Chemical Society). **(B)** Fluorescence images of H_2S and viscosity in *drosophila* brains using probe 5 (reproduced from (Fang et al., 2020) with permission from Elsevier (B. V). **(C)** Fluorescence images of viscosity and H_2S in a zebrafish model of PD using probe **6** (reproduced from (Shen et al., 2021) with permission from Elsevier (B. V). **(D)** Fluorescence images of PC12 cells incubated with probe 7 without or with glutamate pre-treatment (reproduced from (Kong et al., 2021) with permission from the Royal Society of Chemistry). **(E)** Fluorescence images of PC 12 cells induced by Glu using probe 8 (reproduced from (Li S et al., 2022) with permission from Elsevier (B. V).

biocompatibility, and outstanding photophysical properties (Liu and Tang, 2020; Wu and Liu, 2021; Dai et al., 2022; Li Z et al., 2022). In 2022, Ramya et al. reported a tetraphenylethylene (TPE) "double-locked" fluorescent probe **3**. The TPE fluorophore served as the core structure of AIEgen, 7-nitro-1,2,3-benzoxadiazole (NBD) acted as the recognition site for H_2S, and the disulfide donor generated H_2S in the presence of Cys or GSH. Probe **3** had the advantages of water solubility, low detection limit, and good selectivity for H_2S. Figure 3C displayed that the structure of probe **3** could act as an H_2S donor for subsequent depolymerization of $A\beta_{1\text{-}42}$ protein, limiting the development of AD. In the presence of probe **3**, the toxic aggregated $A\beta_{1\text{-}42}$ peptide became non-toxic disaggregated $A\beta_{1\text{–}42}$. Fluorescent probes with a "double-lock" sequential activation strategy have higher specificity and accuracy compared to the previous "single-lock" probe strategies (Liu et al., 2019).

3.1.2 Parkinson's disease imaging

Parkinson's disease (PD) is characterized by progressive loss of dopaminergic neurons in the substantia nigra (SN) (Hirsch et al., 1988). The first sign of cognitive impairment is memory loss, and then behavioral disturbances (Gagliardi and Vannini, 2022). It has been reported that H_2S, as an antioxidant, has protective effects on PD by scavenging highly reactive oxygen species (ROS) as an antioxidant (Kimura and Kimura, 2004; Kimura et al., 2005). As well, overexpression of CBS or use of H_2S donors offers neuroprotection in a 6-hydroxytryptamine (6-OHDA)-induced PD model (Yin et al., 2017; Cao X et al., 2018). Therefore, studying the pathogenesis of PD will be helpful for early therapy and intervention to slow down the progression of PD in the elderly.

Two-photon microscopy (TPM) exhibits many wonderful merits, including larger penetration depth (>500 μm), localization of excitation, and longer observation time (Xu et al., 2020; Juvekar et al., 2021). In 2013, Kim's group reported a ratiometric two-photon (TP) fluorescent probe (**4**) for testing H_2S in mitochondria, in which 6-(benzo[*d*]thiazol-2′-yl)-2-(methylamino)naphthalene was used as the probe fluorophore, 4-azidobenzyl carbamate was served as the recognition site for H_2S, and triphenylphosphonium salt could be used as the mitochondrial targeting moiety (Bae et al., 2013). When H_2S was added, the emission peaks of probe **4** were red-shifted from 464 to 545 nm. As shown in Figure 4A, the decrease of H_2S and

decrease of CBS expression were observed in studies involving the PD gene DJ-1, in which the decrease of H_2S in astrocytes may facilitate the progress of PD.

Mitochondria, as an important organelle, provides energy for cells, and mitochondrial dysfunction is closely related to PD (Greenamyre, 2018; Grunewald et al., 2019; Doric and Nakamura, 2021). In 2020, Fang and coworkers obtained a TP fluorescent probe **5**, using *N,N*-disubstituted unit as electron donors and pyridine cation as an electron-withdrawing group, which was used for testing mitochondrial viscosity and H_2S (Fang et al., 2020). After different concentrations of H_2S were introduced, the green fluorescence increased significantly. DL-Propargylglycine (PAG, a specific inhibitor of endogenous production of H_2S)-induced PD *Drosophila* brains model had higher viscosity and lower H_2S in mitochondria compared to the normal model (Figure 4B).

Although probe **5** has wonderful selectivity, fine sensitivity, and low detection limit for H_2S, azide, the recognition group of the probe, can be decomposed by UV light, so false signals may be generated. In 2021, Shen and coworkers created a bifunctional near-infrared fluorescence (NIR) probe (**6**), which used dicyanoisopherone as the fluorescence core and 2,4-dinitrobenzenesulfonyl ether as the recognition group of H_2S. Probe **6** had high photostability and a large stokes shift (110 nm). As the augment of H_2S concentration, the fluorescence signal around 650 nm increased 20-fold. Moreover, the fluorescence signal of probe **6** around 580 nm changed with increasing viscosity. The changes in H_2S levels and viscosity were investigated through the experiments of a zebrafish PD model induced by rotenone (a drug to reduce dopamine levels of zebrafish) (Figure 4C). The results showed that both viscosity and H_2S increased in the zebrafish PD model.

Fluorescent probes employing a "double-lock" sequential activation strategy have higher specificity and accuracy compared to single-site release fluorescence (Liu et al., 2019). In 2021, a "double-locked" fluorescent probe **7** for monitoring H_2S in high-viscosity systems was obtained by Kong and coworkers (Kong et al., 2021). In high-viscosity environments (the first "key"), 2,4-dinitrobenzenesulfonate group (the second "key") in probe **7** was recognized with H_2S, and the fluorescence signal around 630 nm was enhanced 50-fold. As shown in Figure 4D, experiments of detecting H_2S and viscosity in glutamate (a neurotoxin)-induced PD PC 12 cell model were conducted. The results showed that the level of H_2S as an antioxidant was upregulated to reduce oxidative stress in glutamate-induced PC12 cells.

Response time is one of the important indicators for the evaluation of probes in biological applications. As shown in Table 1, the reported H_2S fluorescent probes for PD imaging were slow (15–120 min). In 2022, Li S et al. (2022) reported a bifunctional fluorescent probe (**8**) to detect viscosity and H_2S in mitochondria. As viscosity gradually increased, the fluorescence signal of probe **8** around 730 nm was increased. The probe reached a response plateau after the addition of H_2S for 8 min, with a 6-fold amplification of the fluorescence signal around 516 nm. Probe **8** was successfully applied to test the viscosity behavior of a PD model (PC-12 cells treated with glutamate), in which both H_2S and viscosity increased in PD. As shown in Figure 4E, after injection of nystatin or glutamate in nude mouse tumor models, the red fluorescence enhanced notably with time.

3.1.3 Stroke imaging

Ferroptosis (iron-dependent oxidative stress) is closely associated with cancer, neurodegenerative diseases, ischemia-reperfusion injury, etc., and detecting its pathological processes is vital for disease prognosis and treatment (Qiu et al., 2020; Yu et al., 2021; Zhao et al., 2021; Lei et al., 2022; Zhao Y et al., 2022). In 2022, Liang and colleagues reported a NIR fluorescent probe (**9**) with H_2S triggering and H_2S releasing properties. Azidobenzene served as the H_2S recognition site and was linked to the fluorophore *via* thiocarbamate (H_2S precursor). When probe **9** reacted with H_2S, carbonyl sulfide (COS) was released by 1,6-elimination reactions, and then H_2S was released catalyzed by carbonic anhydrase (CA). In glycerol, probe **9** had a strong fluorescence signal at 646 nm. As the H_2S concentration increased, the fluorescence signal around 670 nm increased approximately 25-fold. Moreover, the relationship between oxygen-glucose deprivation/re-oxygenation (OGD/R) and ferroptosis was studied with PC12 cells. Figure 5 showed that the process of cell ischemia-reperfusion was accompanied by ferroptosis and H_2S depletion.

3.2 Inflammation imaging

Inflammation mainly includes two categories, infectious and non-infectious, manifested as swelling, redness, pain, fever, dysfunction, etc (Fontaine et al., 2016). Inflammation is usually beneficial to biological systems, and it is an automatic defense response of biological systems. However, sometimes inflammation can be harmful to tissues and organisms. For example, out-of-control inflammation can be responsible for cardiovascular and cerebrovascular diseases, fibrosis, and cancer (Capuron et al., 2008; Mantovani et al., 2008; Lim, 2018; Mack, 2018; Weiss, Ganz, and Goodnough, 2019). These diseases and inflammation are always mutually reinforcing (Jiang et al., 2019; Majd, Saunders, and Engeland, 2020; Liberale et al., 2022). Therefore, accurate diagnosis at the initial stages of inflammation and preventing the further development of inflammation into more severe diseases is important. H_2S can achieve anti-inflammatory effects by inhibiting the production of inflammatory cytokines, and its overexpression *in vivo* has been considered as a biomarker of all kinds of inflammation. So, it is vital to investigate the behaviors or relationships between H_2S and inflammation in biological systems.

Lipopolysaccharide (LPS), as a dominating cell surface component of Gram-negative bacteria, can be used for bioimaging to induce cellular inflammation models (Lykhmus et al., 2016). In 2021 and 2022, Ou et al. (2021), Ding et al. (2022) fabricated TP fluorescence probes (**10**, **11**) for H_2S imaging in inflammatory models, respectively. Probe **10** consisted of naphthalimide derivative as a fluorophore and 4- dinitrophenyl ether (DNB) as a recognition group. When H_2S existed, probe **10** exhibited amazing fluorescence enhancement (258-fold) at 540 nm. Figure 6A showed that compared with normal tissues, the inflamed tissues had a significant fluorescence signal augmentation in the green channel. Probe **11** consisted of azide and a fluorophore of naphthylimide. When H_2S was introduced, the fluorescence signal around 561 nm was enhanced 38.1-fold. In addition, probe **11** exhibited excellent TP fluorescence properties in cells and liver tissues, penetrating to depths of 126 μm in liver tissue. As shown in Figure 6B, the experiment of the LPS-induced air pouch inflammation model was conducted to observe the development of inflammation and the behavior of H_2S.

In 2021 and 2022, Gong's group and Wang's group fabricated NIR mitochondrial-targeting fluorescent probes (**12**, **13**) for H_2S imaging in inflammatory models, respectively. In probe **12**, the pyridium unit

TABLE 1 Spectroscopic properties and pathophysiological models imaging of small molecular probes for detection of H_2S.

Probe	Pathophysiological models	LOD	$\lambda_{ex}/\lambda_{em}$ (nm)	Response time	Recognition system	Comment	Real sample	References
1	Alzheimer's disease	0.17 μM	370/510	30 min	PBS buffer solution (pH = 7.4)	Dual-response (viscosity and H_2S); mitochondrial targetable; increase in fl. intensity (up to 7-fold)	Living cells	Li et al. (2018)
2	Alzheimer's disease	14.8 nM	540/580	—	PBS buffer solution (pH = 7.4, containing 50% EtOH)	Dual-response (Cu^{2+} and H_2S)	Living cells and living mice	Ma et al. (2019)
3	Alzheimer's disease	0.1 μM	364/480	—	HEPES buffer solution (pH = 7.4, containing 10% THF)	AIE-fluorescence; "double-locked"; increase in fl. intensity (up to 12-fold)	Living cells and living mice	Ramya et al. (2022)
4	Parkinson's disease	0.4 μM	340/500, 420	60 min	HEPES buffer solution (30 mM, pH = 7.4, containing 100 mM KCl)	Two-photon; mitochondrial targetable probe; ratiometric I_{500}/I_{420}	Living cells and tissue	Bae et al. (2013)
5	Parkinson's disease	11.66 nM	480/585	120 min	PBS buffer solution (pH = 7.4, containing 50% DMSO)	Dual-response (viscosity and H_2S); mitochondrial targetable; increase in fl. intensity	Living cells, tissue, and *drosophila* brains	Fang et al. (2020)
6	Parkinson's disease	79 nM	540/650	<15 min	PBS buffer solution (pH = 7.4, containing 1% DMSO)	Dual-response (viscosity and H_2S); large stokes shift (110 nm); NIR imaging; increase in fl. intensity (up to 20-fold)	Living cells, tissue, and living zebra fishes	Shen et al. (2021)
7	Parkinson's disease	0.1 μM	460/630	—	PBS buffer solution (pH = 7.4, containing 10% glycerol)	Dual-response (H_2S and viscosity); "double-locked"; increase in fl. intensity (up to 63-fold)	Living cells	Kong et al. (2021)
8	Parkinson's disease	—	385/516	8 min	PBS buffer solution (pH = 7.4, containing 30% DMSO)	Dual-response (viscosity and H_2S)	Living cells and living mice	Li S et al. (2022)
9	Stroke	1.3 nM	450/670	40 min	PBS buffer solution (pH = 7.4, containing 80% glycerol and 2% DMSO)	NIR imaging; increase in fl. intensity (up to 25-fold)	Living cells and living mice	Liang et al. (2022)
10	Inflammation	18.8 nM	400/540	10 min	PBS buffer solution (10 mM, pH = 7.4, containing 1% DMSO)	Two-photon; increase in fl. intensity (up to 258-fold)	Living cells and tissue	Ou et al. (2021)
11	Inflammation	0.74 μM	440/561	60 min	PBS buffer solution (10 mM, pH = 7.4, containing 1% DMSO)	Two-photon; increase in fl. intensity (up to 38.1-fold)	Living cells, tissue, and living mice	Ding et al. (2022)
12	Inflammation	19 nM	530/663	3 min	PBS buffer solution (10 mM, pH = 7.4)	NIR imaging; large Stokes shift (141 nm); mitochondrial targetable; increase in fl. intensity (up to 27-fold)	Living cells, living zebra fishes, and living mice	Gong et al. (2021)
13	Inflammation	13 nM	540/699	4 min	PBS buffer solution	NIR imaging; large Stokes shift (155 nm); increase in fl. intensity (up to 75-fold)	Living cells, living zebra fishes, and living mice	Wang K et al. (2022)
14	Inflammation	1.8 μM	425/596	10 min	PBS buffer solution (20 mM, pH = 7.4, containing 30% DMF)	Colorimetric; increase in fl. intensity (up to 34-fold)	Living cells and living mice	Hu et al. (2021)
15	Inflammation	310 nM	565/620	120 s	PBS buffer solution	Mitochondrial targetable, increase in fl. intensity (up to 234-fold)	Living cells, living zebra fishes, and living mice	Wang WX et al. (2022)
16	Apoptosis	31 μM	450/540	15 min				Ren M et al. (2021)

(Continued on following page)

TABLE 1 (*Continued*) Spectroscopic properties and pathophysiological models imaging of small molecular probes for detection of H_2S.

Probe	Pathophysiological models	LOD	λ_{ex}/λ_{em} (nm)	Response time	Recognition system	Comment	Real sample	References
					PBS buffer solution (pH = 7.4, containing 30% DMF)	Dual-response (copper II) and H_2S); increase in fl. intensity (up to 40-fold)	Living cells, and living zebra fishes	
17	Apoptosis	—	450/550	45 min	—	Membrane permeability; specific imaging of cancer cells; increase in fl. intensity	Living cells	Singh et al. (2021)
18	Apoptosis	64 nM	–/550	30 min	PBS buffer solution (20 mM, pH = 7.4, containing 5% DMSO)	Increase in fl. intensity	Living cells	Liu et al. (2022)
19	Oxidative Stress	9 μM	–/535	120 min	PBS buffer solution (50 mM, pH = 7.4, containing 0.007% BSA, 100 μM NADH)	Dual-response (hNQO1 and H_2S); "double-locked"; increase in fl. intensity (up to 400-fold)	Living cells	Zhang et al. (2019)
20	Oxidative Stress	0.11 μM	390/515	30 min	PBS buffer solution (10 mM, pH = 7.4, containing 20% DMSO)	Golgi targetable, increase in fl. intensity	Living cells and living zebra fishes	Zhu et al. (2020a)
21	Oxidative stress	0.10 μM	440/550	25 min	PBS buffer solution (10 mM, pH = 7.4)	Golgi targetable, increase in fl. intensity	Living cells and living zebra fishes	Zhu et al. (2020b)
22	Oxidative stress	0.058 μM	325/627, 413	80 min	HEPES buffer (20.0 mM, pH = 7.4, containing 1.0 mM CTAB)	Dual-response (H_2O_2 and H_2S); two increased fluorescence signals	Living cells and living zebra fishes	Yang et al. (2020)
23	Oxidative stress	44.6 nM	460/550	10 min	PBS buffer solution (25 mM, pH = 7.4, containing 30% CH_3CN)	Dual-response (H_2O_2 and H_2S); mitochondrial targetable; "double-locked"; increase in fl. intensity	Living cells and living zebra fishes	Wang Y et al. (2022)
24	Oxidative stress	39.1 nM	480/560, 650	12 min	PBS buffer solution (10 mM, pH = 7.4, containing 10% DMSO)	NIR imaging; large Stokes shift (150 nm); endoplasmic reticulum targetable; ratiometric I_{650}/I_{560}	Living cells and living zebra fishes	Shu et al. (2020)
25	Oxidative stress	17.16 nM	400/464	—	PBS buffer solution (10 mM, pH = 7.4, containing 20% CH_3CN)	Dual-response ($ONOO^-$ and H_2S); increase in fl. intensity	Living cells	Tang et al. (2021)
26	Organ injury	192.1 nM	360/445	15 min	PBS buffer solution (50 mM, pH = 7.4, containing 10% DMF)	Dual-response (HClO and H_2S); two-photon; increase in fl. intensity	Living cells and tissue	Jiao et al. (2018)
27	Organ injury	0.09 μM	720/787	120 min	PBS buffer solution (20 mM, pH = 7.4, containing 5% DMSO)	NIR imaging; increase in fl. intensity (up to 52-fold)	Living cells, living mice , and lung organs	Su et al. (2022)
28	Diabetes	33 nM	600/633	—	PBS buffer solution (20 mM, pH = 7.4)	NIR imaging; "double-locked"; increase in fl. intensity	Living cells and living mice	Li Z et al. (2022)

(positively charged) acted as a mitochondria-targeting group and dinitrophenyl (DNP) ether as an H_2S recognition group. When H_2S was added, a fluorescence-enhancing signal around 663 nm appeared. Probe **12** had the advantages of wonderful water solubility, fast response (<3 min), and large Stokes shift (141 nm). As shown in Figure 6C, changes in H_2S concentration were performed during LPS-induced inflammation in mice. The results suggested that more H_2S could be produced during inflammation. Probe **13** consisted of a NIR fluorophore and a recognition group (NBD). After H_2S was introduced, probe **13** showed a remarkable enhancement (75-fold) in fluorescence signal at 699 nm. Probe **13** exhibited a large Stokes shift (155 nm), quick response (4 min), and wonderful selectivity for H_2S. Probe **13** could detect exogenous and endogenous H_2S in live cells and zebrafish, respectively. Figure 6D showed that probe **13** was used to monitor H_2S fluctuations in LPS-induced inflammatory cells and mice.

Colorimetric detection can be recognized by the naked eye. In 2021, Hu et al. (2021) developed a phenothiazine-based colorimetric

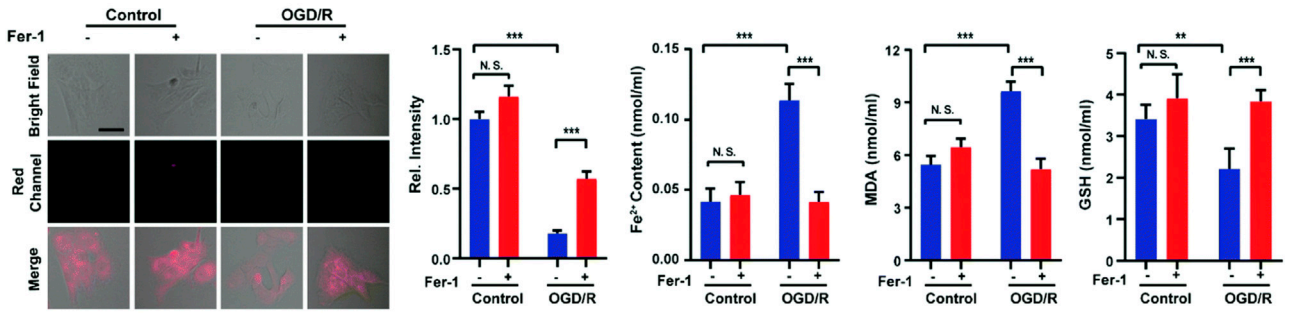

FIGURE 5
Probe 9 for H_2S: High-fidelity ferroptosis evaluation in cells during the stroke (reproduced from (Liang et al., 2022) with permission from the Royal Society of Chemistry).

fluorescence probe (**14**) to selectively detect H_2S in an LPS-induced inflammation mouse model. Probe **14** was based on a donor–π–acceptor (D–π–A) structure that coupled phenothiazine to rhodanine derivative *via* a carbon-carbon double bond. During the probe's identification of H_2S, the fluorescence signal around 596 nm showed a significant increase (34-fold). Probe **14** was able to visualize exogenous and endogenous H_2S *in vitro* and *in vivo* (zebrafish and nude mice). Figure 6E showed that visualization of the production of H_2S in inflammatory models has been realized by probe **14**.

Rhodamine dyes are attracting attention for their wonderful photostability, long emission wavelength, convenient synthesis, and high quantum yield (Rajasekar, 2021). In 2022, Wang and coworkers created a mitochondrial-targeting fluorescent probe **15** to test the changes in H_2S concentration. The fluorescence intensity around 620 nm progressively augmented about 234-fold with increasing H_2S concentration. Probe **15** had some wonderful features of fast response (120 s), low detection limit (310 nM), and excellent sensitivity. Probe **15** could monitor exogenous and endogenous H_2S in HeLa cells and zebrafish, respectively. Probe **15** could be used to visually detect H_2S in LPS-induced mouse inflammation experiments (Figure 6F). And probe **15** was appropriate for testing the behavior of H_2S in human plasma samples.

3.3 Apoptosis imaging

Apoptosis is caused by pathological and physiological conditions triggered by extracellular death receptor ligation or DNA damage and/or cytoskeletal disruption (Akçapınar et al., 2021). The intrinsic way of apoptosis is triggered by the cell's response to injury, while the external way is triggered by cell-stimulated death receptors of the immune system (Sica et al., 1990; Oppenheim et al., 2001). When caspase 3 is activated, both pathways converge, leading to cell death (D'arcy, 2019). Timely monitoring of apoptosis is helpful for early warning and therapy of related pathophysiological processes and the continuous assessment of drug effectiveness. H_2S has been found to protect cells: H_2S can prevent Abeta-induced neuronal apoptosis by diminishing mitochondrial translocation of phosphatase and tensin homolog deleted on chromosome ten (PTEN) (Cui Z et al., 2016); H_2S can restrain cell apoptosis and protect bronchial epithelium in a mouse model of allergic inflammation (Mendes et al., 2019); H_2S improves LPS-induced memory disorder in mice by decreasing apoptosis, oxidation, and inflammatory effects (Kshirsagar et al., 2021). However, H_2S can also promote apoptosis: H_2S contributes to LPS-induced osteoblast apoptosis by restraining the AKT/NF-κB signaling pathway (Wang et al., 2020); H_2S, which releases whey protein derivatives, induces apoptosis through extrinsic and intrinsic pathways (Li et al., 2020). Therefore, the exact relationship between H_2S and apoptosis needs to be further studied.

Cu/NaHS significantly reduced the Menkes copper transport (ATP7A) protein levels, promoted intracellular Cu accumulation, and resulted in increased Cu cytotoxicity (Goto et al., 2020). Therefore, continuous detection of H_2S and Cu^{2+} is helpful to understand their interaction. In 2021, a bifunctional fluorescent probe (**16**) for testing H_2S and Cu^{2+} in different channels in live cells and zebrafish was reported by Ren and colleagues. Naphthalimide and rhodamine were used as probe fluorophores, and azide and hydralazine were selected as recognition sites for H_2S and Cu^{2+}. The fluorescence intensity augmented 40-fold and 31-fold in response to H_2S and Cu^{2+}, respectively. Probe **16** allowed simultaneous fluorescence imaging of H_2S and Cu^{2+} in cells, enabling visualization of H_2S-enhanced Cu^{2+} cytotoxicity (Figure 7A).

In 2021, Singh et al. fabricated a naphthalimide-based bifunctional fluorescent probe **17** for detecting H_2S, which was made up of a peptide-naphthalimide fluorophore and an H_2S sensing moiety. When H_2S was introduced, the morphology of probe **17** showed the combination of fibrous "bushes" with bright yellow fluorescence. Probe **17** had the ability of cancer cell imaging and induction of apoptosis in the meantime, which could be a good candidate for the theranostic agent (Figure 7B).

Because of its fascinating optical properties, including large Stokes shift, "turn-on" fluorescence, relatively high quantum yield, and good photostability, 3-hydroxyflavone has been widely concerned by researchers (Sedgwick et al., 2018; Wang, Lai, Qiu and Liu, 2019; Doric and Nakamura, 2021). In 2022, Liu et al. (2022) created a fluorescent probe **18** based on excited state intramolecular proton transfer (ESIPT) for testing H_2S. The probe consisted of 3-hydroxyflavone and 4-Chloro-7-nitro-1,2,3-benzoxadiazole (NBD-Cl, H_2S-specific recognition unit). When H_2S existed, 3-hydroxyflavone formed a ketone tautomer and released fluorescence at 550 nm. Figure 7C showed the behavior of different concentrations of H_2S on the apoptosis of MCF-7 cells.

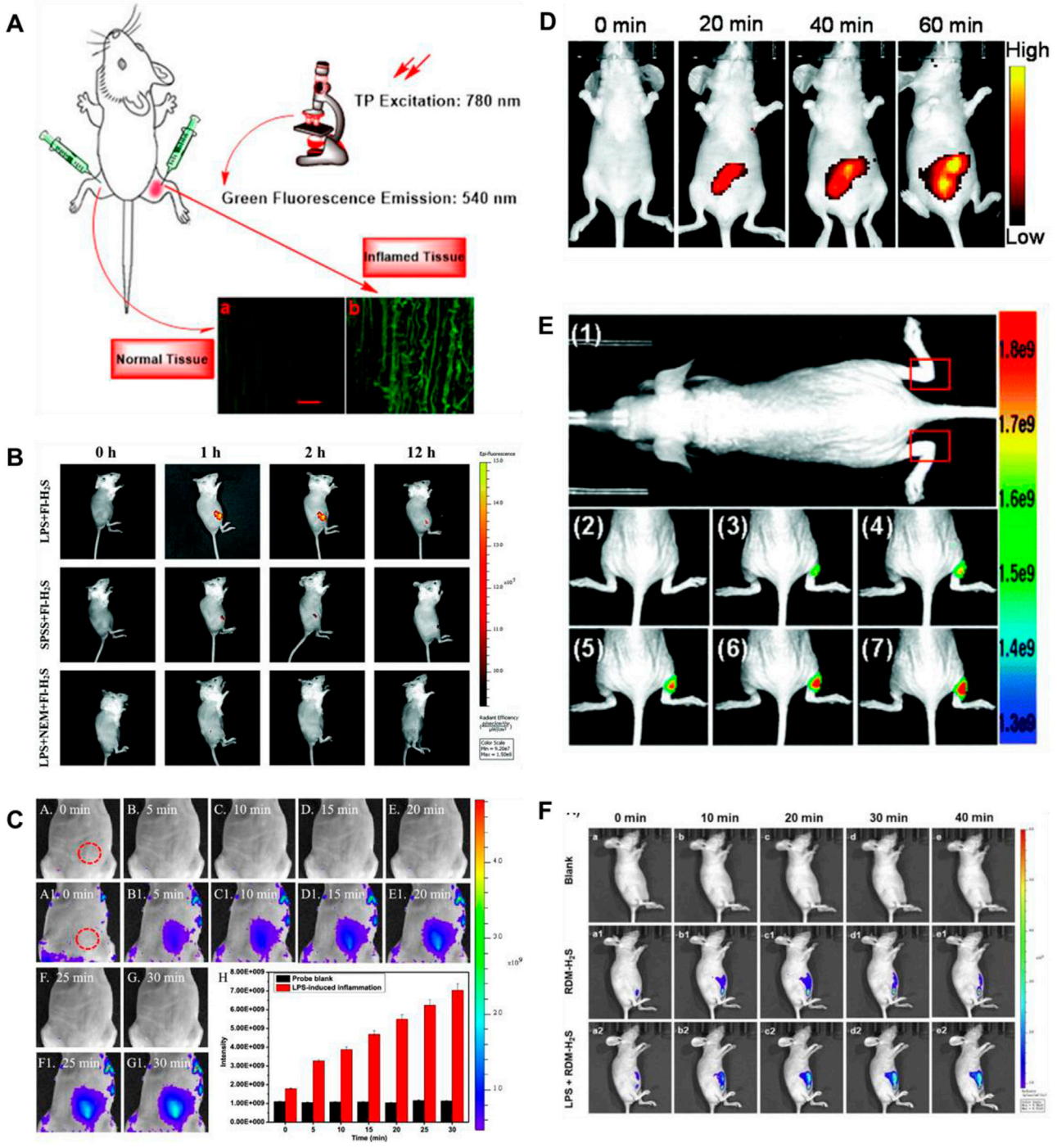

FIGURE 6
(A) Images of a frozen inflamed and normal tissue slice from Kunming mouse using probe 10 (reproduced from (Ou et al., 2021) with permission from Elsevier (B. V). **(B)** Time-dependent fluorescence images of air pouch inflammation in a female nude mouse before and after subcutaneous injection of probe 11 (reproduced from (Ding et al., 2022) with permission from the Royal Society of Chemistry). **(C)** Imaging of H_2S during the LPS-induced inflammation in mice using probe 12 (reproduced from (Gong et al., 2021) with permission from American Chemical Society). **(D)** Fluorescence images of H_2S in the inflammation mice model using probe 13 (reproduced from (Wang Y et al., 2022) with permission from the Royal Society of Chemistry). **(E)** Fluorescence images of H_2S generation in an inflammation model in live nude mice using probe 14 (reproduced from (Hu et al., 2021) with permission from the Royal Society of Chemistry). **(F)** Fluorescence imaging of probe 15 in LPS-induced inflammatory processes in living mice (reproduced from (Wang WX et al., 2022) with permission from Elsevier (B. V).

3.4 Oxidative stress imaging

The imbalance between oxidants and antioxidants is beneficial to oxidants and can cause damage, known as oxidative stress (Sies, 1997). Oxidants are normal products of aerobic metabolism, but they can be produced at a higher rate under pathophysiological conditions. If left unchecked, oxidative stress can lead to damage to DNA, proteins, and lipids, and ultimately cell death (Greenwood and Witney, 2021). H_2S

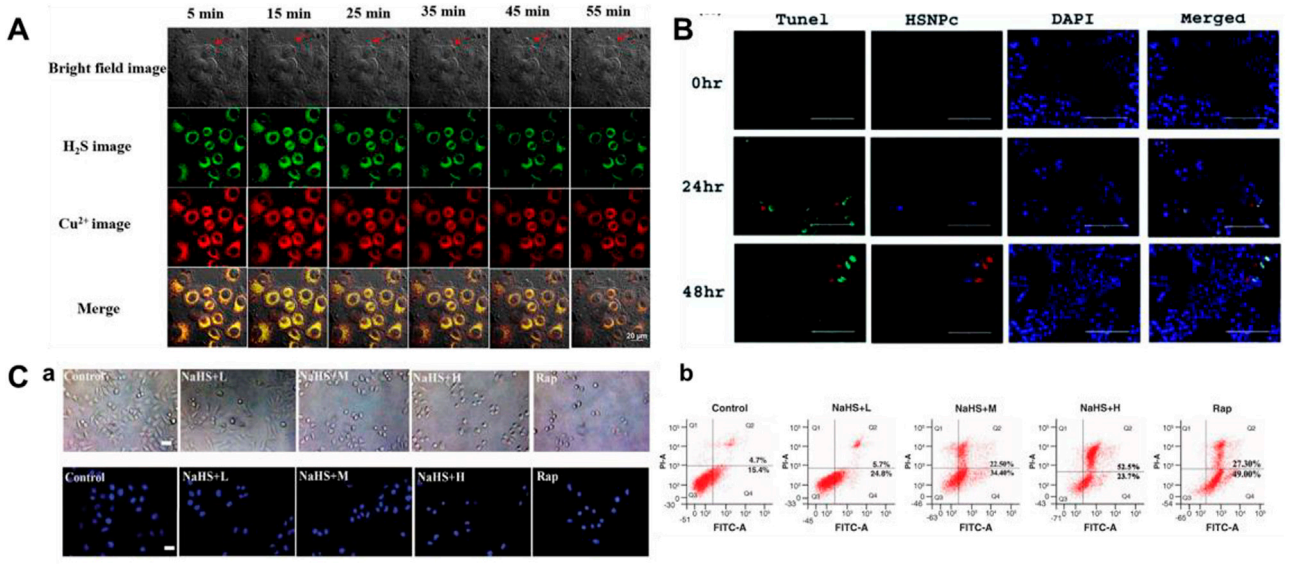

FIGURE 7
(A) Simultaneous fluorescent images of copper (II) ions and H_2S in HeLa cells stained with probe 16 and treated with $CuSO_4$ and NaHS at different times (reproduced from (Ren M et al., 2021) with permission from Elsevier (B. V). **(B)** Determination of apoptosis by TUNEL assay using probe 17 (reproduced from (Singh et al., 2021) with permission from the Royal Society of Chemistry). **(C)** Apoptosis induced by H_2S leads to decrease in cell viability using probe 18 (reproduced from (Liu et al., 2022) with permission from Newlands Press).

has been proven to influence cellular redox through multiple mechanisms, such as ROS scavenging, protein modification, mitochondria, and respiratory oxidation (Pal, Bandyopadhyay, and Singh, 2018; Scammahorn et al., 2021). Furthermore, some suborganelles are related to oxidative stress, for example, the Golgi apparatus actively participates in the stress response, and when larger than the stress threshold, the Golgi apparatus can simultaneously activate cell repair and apoptosis mechanisms (Hicks and Machamer, 2005; Wlodkowic, Skommer, Mcguinness, Hillier, and Darzynkiewicz, 2009); H_2S can effectively decrease endothelial-mesenchymal conversion by restraining ER stress (Ying et al., 2016). Therefore, tracking H_2S behaviors in different organelles is crucial for the research and treatment of related diseases or pathophysiological processes.

H_2S and human NAD(P)H:quinine oxidoreductase 1 (hNQO1), as latent cancer biomarkers, were able to participate in cell redox homeostasis (Park, et al., 2021). In 2019, Zhang et al. (2019) developed a dual biomarker (H_2S and hNQO1)-triggered fluorescent probe to reveal the synergistic antioxidant effect under oxidative stress. Quinone propionic acid (Q_3PA) and NBD served as hNQO1 and H_2S recognition units, and coumarin and naphthalimide acted as fluorophores of probe **19**, respectively. The strategy of dual reaction and dual quenching was formed, which improved the sensitivity and selectivity of the probe. When H_2S existed, the fluorescence signal of probe **19** was remarkably enhanced (400-fold) at 535 nm. In addition, the probe could simultaneously test the endogenous H_2S and hNQO1 activities in organic systems. Figure 8A showed that HeLa cells could induce the production of endogenous H_2S under the existence of exogenous hydrogen peroxide (H_2O_2), that is, H_2S played a synergistic antioxidant role under oxidative stress.

The Golgi stress response is activated when Golgi function is inadequate compared to cellular demands (Gao, et al., 2021). Golgi apparatus provides cytoprotection by moderating the synthesis and metabolism of bioactive molecules in response to conventional stress (Paul, et al., 2014; Hirayama, et al., 2019). In 2020, Zhu et al. (2020), Shu et al. (2020) reported Golgi-targeted fluorescent probes (**20**, **21**) detecting H_2S, respectively. In probe **20**, 4-CF_3-substituted 7-aminoquinoline was used as fluorophore, and azide was elected as the specific identification group of H_2S. The introduction of trifluoromethyl into the quinoline structure facilitated the entry of the probe into the Golgi apparatus through the membrane barrier. With the H_2S concentration increased, the fluorescence signal around 515 nm was augmented. As shown in Figure 8B, probe **20** has achieved *in situ* display of H_2S generation under monensin-induced Golgi pressure. In probe **21**, 1,8-naphthalimide was used as the fluorophore, azide was used as the identification group of H_2S, and phenylsulfonamide was used as the targeting group of the Golgi apparatus. When H_2S was introduced, the fluorescence signal was remarkably enhanced at 550 nm. Furthermore, Figure 8C showed probe **21** could be seen as a chemical method to detect the behavior of H_2S *in situ* during Golgi stress, thus confirming that H_2S could be used as a biomarker to investigate Golgi stress.

Intracellular H_2S and H_2O_2 are closely associated with maintaining cellular homeostasis, and their levels directly reflect the degree of oxidative stress and disease (Kimura and Kimura, 2004; Kimura, et al., 2009). In 2020, Yang et al. (2020) fabricated a fluorescent probe **22** for testing dynamic H_2O_2/H_2S redox processes in organisms. Phenylboronate and azide moieties served as recognition units for H_2O_2 and H_2S, respectively. Under the existence of H_2O_2, the fluorescence intensity around 413 nm declined, while the fluorescence around 486 nm enhanced remarkably. When H_2S was added, two fluorophores (HCB and TQC) were released, and the fluorescence at 413 and 627 nm were emitted, respectively. Figure 8D showed phorbol 12-myristate 13-acetate (PMA)-induced stress experiments, in which cells produced H_2O_2 and reduced H_2S. In 2022, Wang and colleagues

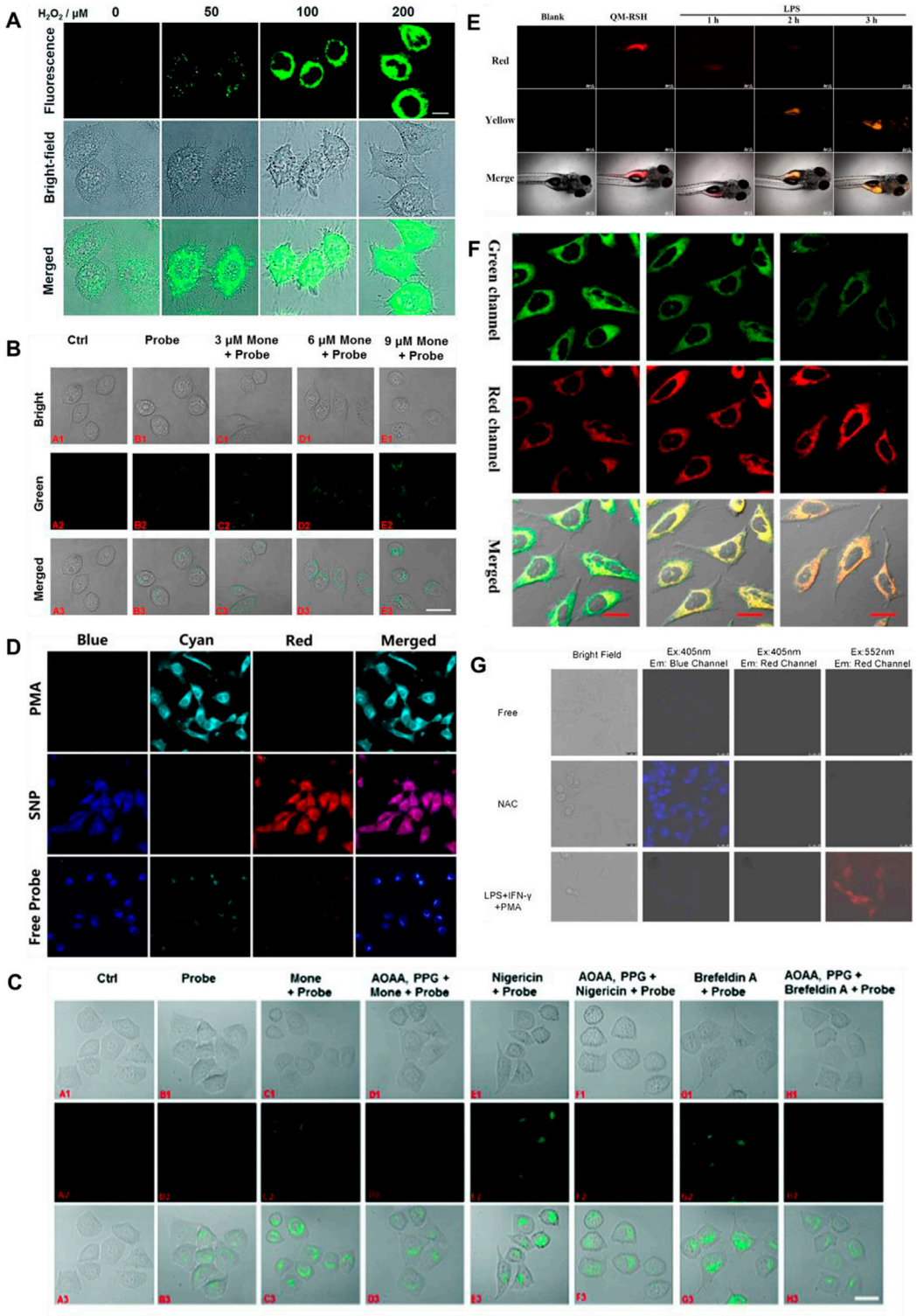

FIGURE 8
(A) Confocal microscopy images for concentration-dependent H_2O_2-induced fluorescence in living HeLa cells using probe 19 (reproduced from (Zhang et al., 2019) with permission from the Royal Society of Chemistry). **(B)** Golgi stress response experiments in cells using probe 20 (reproduced from (Zhu et al., 2020a) with permission from American Chemical Society). **(C)** Fluorescence imaging of probe 21 after stimulating cells with only probe 22, Mone, aminooxyacetic acid (AOAA)/photoplethysmographic (PPG) Mone, nigericin, AOAA/PPG/igericin, brefeldin A, and AOAA/PPG/brefeldin A, respectively (reproduced from (Zhu et al., 2020b) with permission from the Royal Society of Chemistry). **(D)** Confocal fluorescence images of endogenous H_2O_2/H_2S in living HeLa cells using probe 22 (reproduced from (Yang et al., 2020) with permission from American Chemical Society). **(E)** Fluorescence imaging H2S in inflammation response zebrafish using probe 23 (reproduced from (Wang K et al., 2022) with permission from Elsevier (B. V). **(F)** Confocal imaging of H_2S during ER stress with probe 24 (reproduced from (Shu et al., 2020) with permission from American Chemical Society). **(G)** HUEVC cells imaging endogenous $ONOO^-$ and H_2S using probe 25 (reproduced from (Tang et al., 2021) with permission from Elsevier (B. V).

obtained a NIR fluorescence probe activated by H_2O_2 to monitor the changes in H_2S during oxidative stress. When H_2O_2 was present, the fluorescence signal of probe **23** blue-shifted from 700 to 550 nm after recognizing H_2S. Probe **23** could monitor the changes in H_2S during the oxidation-triggered oxidative stress process in cells and zebrafish. Figure 8E showed that the probe evaluated the up-regulation of H_2S levels based on oxidative stress by H_2O_2/PMA.

The endoplasmic reticulum (ER) plays a critical role in protein synthesis, folding, distribution, and storage of calcium ions (BÁnhegyi, et al., 2007; Pagliassotti, et al., 2016). ER stress can result in autophagy and even cell death, which is bound up with serious diseases or pathophysiological processes (Holczer, et al., 2018). In 2020, Shu et al. (2020) reported an ER-targeted ratiometric fluorescent probe for detecting H_2S in organism systems. Probe **24** was composed of dicyanoisophorone analogue with a large Stokes shift and *o*-carboxybenzaldehyde as the specific recognition group of H_2S. H_2S reacted with the aldehyde group in the probe through nucleophilic addition, emitting fluorescence at 650 nm. The probe had good selectivity, large Stokes shift (150 nm). Figure 8F showed that the probe observed the endogenous changes in H_2S under tunicamycin-induced endoplasmic reticulum stress.

Abnormal metabolism of organisms produces high concentrations of active carbonyl substances, leading to carbonyl stress, which leads to cell injury or cell apoptosis (Bordoni, et al., 2006). Therefore, the development of tools to image carbonyl stress is essential to decrease its damage and explore new drug treatments or reduce carbonyl stress. In 2021, a visualized fluorescent probe (**25**) for monitoring the protective effect of endogenous H_2S during carbonyl stress in endothelial cells was developed by Tang and colleagues. The probe had dual fluorophores (rhodamine and coumarin fluorophores) and dual recognition sites (phenylhydrazine and 2,4-dinitrobenzenesulfonyl ether) to achieve the purpose of dual recognition of H_2S and $ONOO^-$, and the fluorescence signals of rhodamine and coumarin would not interfere with each other (>100 nm). When H_2S and $ONOO^-$ were introduced, the probe showed remarkable increases in fluorescence signal around 464 and 570 nm, respectively. Probe **25** enabled endogenous H_2S and $ONOO^-$ imaging in different channels. Figure 8G showed that probe **25** was suitable for visualizing the protective effect of endogenous H_2S during carbonyl stress.

3.5 Organ injury imaging

H_2S is synthesized in almost all organ systems (Kasinath et al., 2018). H_2S has been proven to protect against organ damage, including liver damage, heart damage, kidney damage, etc (Tan et al., 2011; Wang et al., 2012; Kasinath, 2014). For example, in acute or chronic kidney disorders, H_2S generation from the renal cells is decreased (Koning et al., 2015; Lobb et al., 2015; Cao and Bian, 2016; Cao et al., 2019); Endogenous and exogenous H_2S reduces myocardial damage and improves cardiac function (Johansen et al., 2006; Wu et al., 2021); Decreased levels of endogenous H_2S in the brain were associated with increased lesion volume and mortality after traumatic brain injury (TBI) (Zhang et al., 2013); H_2S prevents LPS-induced acute lung injury (ALI) by restraining synergistic pro-inflammatory and oxidative reactions of stress proteins, mitogen-activated protein kinases (MAP kinases), and ROS signaling pathways (Zimmermann et al., 2018). Therefore, the development of sensitive probes for *in vivo* imaging of H_2S is critical for exploring H_2S biology and the diagnosis of organ injury.

In 2018, Jiao's group developed a TP fluorescent probe **26**, which was used to explore the potency of HClO as an indicator of drug-induced liver injury (DILI) and the detoxification of N-acetylcysteine (NAC) mediated by H_2S. The probe was linked by 7-amino coumarin and rhodamine B *via* piperazine. When HClO or H_2S existed, the fluorescence signal was remarkably enhanced at 580 or 445 nm. In this process, the recovery of the D-π-A structure induced by azide reduction of H_2S and the ring opening induced by HClO were carried out separately, so that H_2S and HClO did not generate signals that interfered with each other. As shown in Figure 9A, DILI induced by antidepressants such as duloxetine and fluoxetine and their remission were assessed at the cellular and tissue levels, respectively. The data showed that only after combined administration of the drugs, a significant increase of HClO and significant liver injury were found. At the same time, NAC pretreatment led to an increase in endogenous H_2S levels, which was helpful in the remission of DILI.

Hemicyanine dyes have great potential in the research of small animal imaging and disease modeling owing to their emission in the NIR regions, convenient synthesis, and wavelength tunability (Li H et al., 2022). In 2022, a NIR fluorescent probe **27** based on sulfur-substitution hemicyanine dye for H_2S recognition was obtained by Su and colleagues. In contrast to traditional hemicyanine dyes, the oxygen in oxygen-substitution hemicyanine dyes was substituted by sulfur to become sulfur-substitution hemicyanine dyes. 2,4-dinitrophenyl served as the identifying site for H_2S and the quenching group for probe fluorescence. As H_2S concentration increases, the fluorescence signal around 787 nm was markedly increased (52-fold), red-shifted by 60 nm compared to oxygen-substituted hemicyanine dyes. As shown in Figure 9B, in the mouse model experiment of LPS-induced acute lung injury, the data showed a significant increase in H_2S concentration.

3.6 Diabetic imaging

Diabetes, as a disease characterized by hyperglycemia, is related to diverse complications, including cardiovascular disease, stroke, kidney failure, neuropathy, retinopathy, and amputation (Al-Sofiani et al., 2019; Lau et al., 2019; Buades et al., 2021; Sempere-Bigorra et al., 2021; Milluzzo et al., 2021; O'neill et al., 2017). It is reported that diabetes can be divided into three types: Gestational diabetes, type 1 diabetes (T1D), and type 2 diabetes (T2D) (Xiang et al., 2018). H_2S, as a promising candidate, helps to prevent and therapy of diabetes (Sun et al., 2021). Compared to lean participants, overweight and T2D patients had significantly lower blood levels of H_2S (Whiteman et al., 2010). The protein expression and activity of CSE were significantly higher in peripheral blood mononuclear cells of normal humans than T1D patients (Manna et al., 2014). Therefore, studying the relationship between H_2S and diabetes in-depth may be helpful to develop potential treatments for diabetes.

In 2022, a "double-locked" fluorescent probe **28** with NIR emission for examining the H_2S levels in organisms was obtained by Wei and colleagues. Probe **28** consisted of a fluorophore with NIR emission (rhodamine B), and re-active units of H_2S (aromatic azide

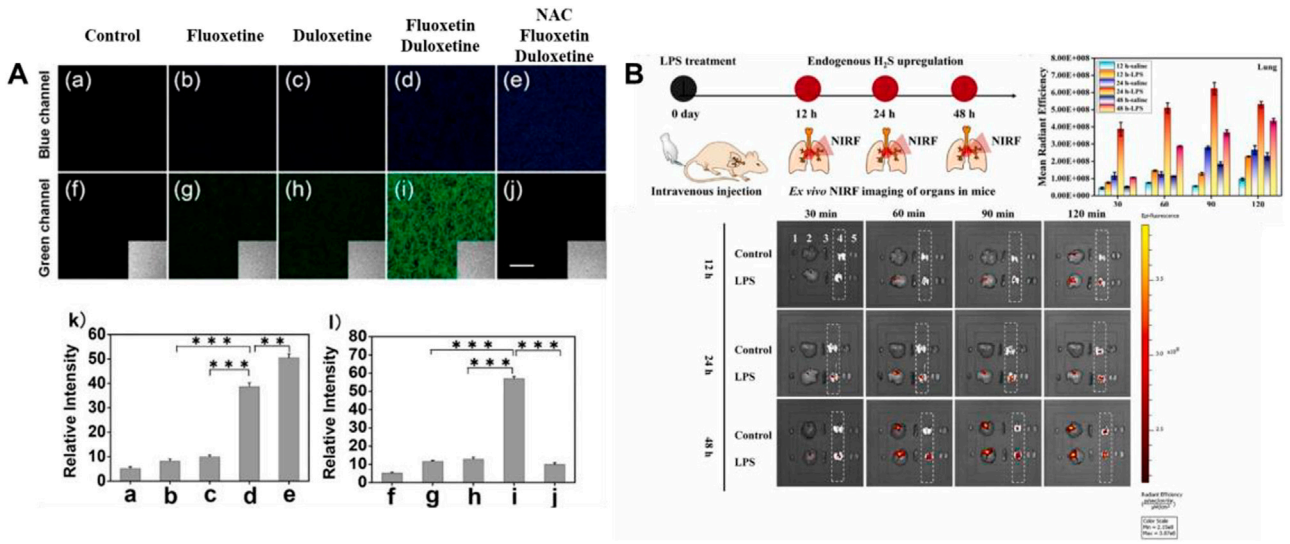

FIGURE 9
(A) TPM imaging of endogenous H_2S and HClO in RAW264.7 cells upon drug treatment using probe 26 (reproduced from (Jiao et al., 2018) with permission from American Chemical Society). **(B)** Schematic illustration of probe 27 reporting the H_2S upregulation process in ALI mice's lungs (reproduced from (Su et al., 2022) with permission from Elsevier (B. V).

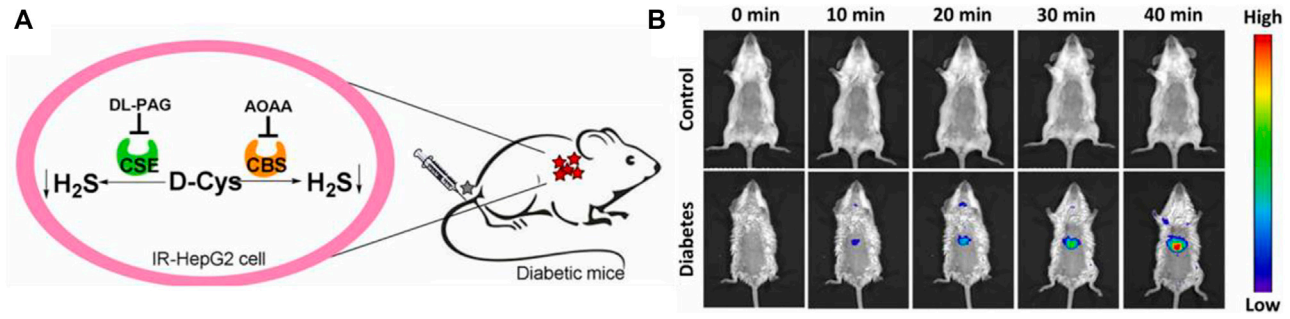

FIGURE 10
(A) Endogenous H_2S biosynthesis in IR-HepG2 cells. **(B)** Fluorescence imaging of control (up) and diabetic (down) mice using probe 28 (reproduced from (Li Z et al., 2022) with permission from Elsevier (B. V).

and NBD-piperazine). The fluorescence around 663 nm was locked and quenched through the intramolecular charge transfer (ICT) and photoinduced electron transfer (PET) processes. Probe **28** exhibited good selectivity and excellent sensitivity for imaging the behaviors of H_2S. In addition, probe 28 was applied to image the levels of endogenous H_2S in IR-Hepg2 cells and diabetic mice (Figure 10).

4 Summary and outlook

Fluorescence imaging may become a universally accepted diagnostic modality in the future due to its high efficiency and low cost. Accurate detection of H_2S associated with pathophysiological processes and examining their behaviors are essential for understanding the diseases or pathophysiological processes involved, especially in the early stages. This paper reviews the bioimaging of H_2S in pathophysiological processes (neurodegenerative diseases, inflammation, apoptosis, oxidative stress, organ injury, and diabetes) with fluorescent diagnostic probes. The design strategies, recognition mechanisms, optical properties, and applications of H_2S fluorescent probes in bioimaging are further discussed. Up to now, remarkable progress has been achieved in exploring organic fluorescent probes for examining and studying H_2S-associated pathophysiological processes in real-time.

Although delightful progress has been obtained, there are still some issues that need to be improved and solved: 1) Most fluorescent probes are inherently monochromatic, which can easily lead to false-positive signals in complex physiological settings, resulting in incorrect disease diagnosis; 2) Most H_2S fluorescent probes reported to date have fluorescence emission wavelengths in the UV-visible region, which limits their application in studying diseases. There is still a large lack of H_2S-based organic fluorescent probes that can be applied for routine diagnosis and monitoring of clinical diseases or pathophysiological processes. So it is crucial and

urgent to construct novel fluorescent probes with fascinating advantages for imaging H_2S associated with pathophysiological processes. To achieve this goal, we can start from the following aspects: 1) Designing fluorescent probes with excellent properties, including high quantum yields, large Stokes shifts, large photostability, and fast response; 2) Exploring the fluorescent probes of H_2S with fine tissue penetration and high spatial resolution, which may have the greatest application due to the depth of biological tissues; 3) Developing organic fluorescent probes in the NIR-II region, which is expected to facilitate the development of systems suitable for monitoring deep organ-related diseases.

Overall, organic fluorescent probes with wonderful features might have the ability to image H_2S associated with pathophysiological processes. It is believed that organic fluorescent probes for imaging H_2S in pathophysiological processes will become increasingly vital testing tools in the future.

Author contributions

T-TJ: writing—original draft; literature collection. YZ: literature collection. HN: literature collection; processing of pictures. J-TH: conceptualization; supervision; editing. SW: supervision; methodology. All authors contributed to the article and approved the submitted version. All authors listed have made a substantial, direct, and intellectual contribution to the work and approved it for publication.

Funding

This research was funded by the National Natural Science Foundation of China (No. 22207087) and the Natural Science Foundation of Henan (No. 222300420244).

Conflict of interest

The authors declare that the research was conducted in the absence of any commercial or financial relationships that could be construed as a potential conflict of interest.

Publisher's note

References

Akçapınar, R., Garipcan, B., Goodarzi, V., and Uzun, L. (2021). Designing of various biosensor devices for determination of apoptosis: A comprehensive review. *Biochem. Biophys. Res. Commun.* 578, 42–62. doi:10.1016/j.bbrc.2021.08.089

Al-Sofiani, M. E., Derenbecker, R., Quartuccio, M., and Kalyani, R. R. (2019). Aspirin for primary prevention of cardiovascular disease in diabetes: A review of the evidence. *Curr. Diab. Rep.* 19, 107. doi:10.1007/s11892-019-1206-6

Antequera, T., Caballero, D., Grassi, S., Uttaro, B., and Perez-Palacios, T. (2021). Evaluation of fresh meat quality by hyperspectral imaging (HSI), nuclear magnetic resonance (nmr) and magnetic resonance imaging (MRI): A review. *Meat Sci.* 172, 108340. doi:10.1016/j.meatsci.2020.108340

Augsburger, F., and Szabo, C. (2020). Potential role of the 3-mercaptopyruvate sulfurtransferase (3-mst)-hydrogen sulfide (H_2S) pathway in cancer cells. *Pharmacol. Res.* 154, 104083. doi:10.1016/j.phrs.2018.11.034

Austgen, J. R., Hermann, G. E., Dantzler, H. A., Rogers, R. C., and Kline, D. D. (2011). Hydrogen sulfide augments synaptic neurotransmission in the nucleus of the solitary tract. *J. Neurophysiol.* 106, 1822–1832. doi:10.1152/jn.00463.2011

Bae, S. K., Heo, C. H., Choi, D. J., Sen, D., Joe, E. H., Cho, B. R., et al. (2013). A rratiometric two-photon fluorescent probe reveals reduction in mitochondrial H_2S production in Parkinson's disease gene knockout astrocytes. *J. Am. Chem. Soc.* 135, 9915–9923. doi:10.1021/ja404004v

Bánhegyi, G., Baumeister, P., Benedetti, A., Dong, D., Fu, Y., Lee, A. S., et al. (2007). Endoplasmic reticulum stress. *Ann. N. Y. Acad. Sci.* 1113, 58–71. doi:10.1196/annals.1391.007

Bełtowski, J., Wójcicka, G., and Jamroz-Wiśniewska, A. (2018). Hydrogen sulfide in the regulation of insulin secretion and insulin sensitivity: Implications for the pathogenesis and treatment of diabetes mellitus. *Biochem. Pharmacol.* 149, 60–76. doi:10.1016/j.bcp.2018.01.004

Bordoni, V., Piroddi, M., Galli, F., De Cal, M., Bonello, M., Dimitri, P., et al. (2006). Oxidant and carbonyl stress-related apoptosis in end-stage kidney disease: Impact of membrane flux. *Blood Purif.* 24, 149–156. doi:10.1159/000089452

Buades, J. M., Craver, L., Del Pino, M. D., Prieto-Velasco, M., Ruiz, J. C., Salgueira, M., et al. (2021). Management of kidney failure in patients with diabetes mellitus: What are the best options? *J. Clin. Med.* 10, 2943. doi:10.3390/jcm10132943

Cao, X., and Bian, J. S. (2016). The role of hydrogen sulfide in renal system. *Front. Pharmacol.* 7, 385. doi:10.3389/fphar.2016.00385

Cao, L., Cao, X., Zhou, Y., Nagpure, B. V., Wu, Z. Y., Hu, L. F., et al. (2018). Hydrogen sulfide inhibits ATP-induced neuroinflammation and Aβ1–42 synthesis by suppressing the activation of STAT3 and cathepsin S. *Brain Behav. Immun.* 73, 603–614. doi:10.1016/j.bbi.2018.07.005

Cao, X., Cao, L., Ding, L., and Bian, J.-S. (2018). A new hope for a devastating disease: Hydrogen sulfide in Parkinson's disease. *Mol. Neurobiol.* 55, 3789–3799. doi:10.1007/s12035-017-0617-0

Cao, X., Zhang, W., Moore, P. K., and Bian, J. (2019). Protective smell of hydrogen sulfide and polysulfide in cisplatin-induced nephrotoxicity. *Int. J. Mol. Sci.* 20, 313. doi:10.3390/ijms20020313

Capuron, L., Su, S., Miller, A. H., Bremner, J. D., Goldberg, J., Vogt, G. J., et al. (2008). Depressive symptoms and metabolic syndrome: Is inflammation the underlying link? *Biol. Psychiatry* 64, 896–900. doi:10.1016/j.biopsych.2008.05.019

Chan, S. J., and Wong, P. T. H. (2017). Hydrogen sulfide in stroke: Protective or deleterious? *Neurochem. Int.* 105, 1–10. doi:10.1016/j.neuint.2016.11.015

Cirino, G., Szabo, C., and Papapetropoulos, A. (2022). Physiological roles of hydrogen sulfide in mammalian cells, tissues, and organs. *Physiol. Rev.* 103, 31–276. doi:10.1152/physrev.00028.2021

Cui, W., Zhang, Y., Yang, C., Sun, Y., Zhang, M., and Wang, S. (2016). Hydrogen sulfide prevents abeta-induced neuronal apoptosis by attenuating mitochondrial translocation of PTEN. *Neuroscience* 325, 165–174. doi:10.1016/j.neuroscience.2016.03.053

Cui, Z., Bu, W., Fan, W., Zhang, J., Ni, D., Liu, Y., et al. (2016). Sensitive imaging and effective capture of Cu^{2+}: Towards highly efficient theranostics of alzheimer's disease. *Biomaterials* 104, 158–167. doi:10.1016/j.biomaterials.2016.06.056

Dai, J., Xue, H., Chen, D., Lou, X., Xia, F., and Wang, S. (2022). Aggregation-induced emission luminogens for assisted cancer surgery. *Coord. Chem. Rev.* 464, 214552. doi:10.1016/j.ccr.2022.214552

D'arcy, M. S. (2019). Cell death: A review of the major forms of apoptosis, necrosis and autophagy. *Cell. Biol. Int.* 43, 582–592. doi:10.1002/cbin.11137

Ding, D., Li, J., Xu, L., Wang, J., Tan, D., and Lin, W. (2022). Development of an activatable hydrogen sulfide-specific two-photon fluorescent probe for bioimaging in an air pouch inflammation model. *J. Mat. Chem. B* 10, 4568–4574. doi:10.1039/d2tb00681b

Disbrow, E., Stokes, K. Y., Ledbetter, C., Patterson, J., Kelley, R., Pardue, S., et al. (2021). Plasma hydrogen sulfide: A biomarker of alzheimer's disease and related dementias. *Alzheimers Dement.* 17, 1391–1402. doi:10.1002/alz.12305

Doric, Z., and Nakamura, K. (2021). Mice with disrupted mitochondria used to model Parkinson's disease. *Nature* 599, 558–560. doi:10.1038/d41586-021-02955-z

Du, H., Zhang, H., Fan, Y., Zheng, Y., Yuan, S., Jia, T.-T., et al. (2023). A novel fluorescent probe for the detection of formaldehyde in real food samples, animal serum samples and gaseous formaldehyde. *Food Chem.*, 135483. doi:10.1016/j.foodchem.2023.135483

Fang, Z., Su, Z., Qin, W., Li, H., Fang, B., Du, W., et al. (2020). Two-photon dual-channel fluorogenic probe for *in situ* imaging the mitochondrial H_2S/viscosity in the brain of Drosophila Parkinson's disease model. *Chin. Chem. Let.* 31, 2903–2908. doi:10.1016/j.cclet.2020.03.063

Fontaine, M., Lepape, A., Piriou, V., Venet, F., and Friggeri, A. (2016). Innate danger signals in acute injury: From bench to bedside. *Anaesth. Crit. Care Pa.* 35, 283–292. doi:10.1016/j.accpm.2015.10.009

Gagliardi, G., and Vannini, P. (2022). Episodic memory impairment mediates the loss of awareness in mild cognitive impairment. *Front. Aging Neurosci.* 13, 802501. doi:10.3389/fnagi.2021.802501

Gao, J., Gao, A., Liu, W., and Chen, L. (2021). Golgi stress response: A regulatory mechanism of Golgi function. *BioFactors* 47, 964–974. doi:10.1002/biof.1780

Gardner, S. H., Reinhardt, C. J., and Chan, J. (2021). Advances in activity-based sensing probes for isoform-selective imaging of enzymatic activity. *Angew. Chem. Int. Ed.* 60, 5000–5009. doi:10.1002/anie.202003687

Gong, S., Zheng, Z., Guan, X., Feng, S., and Feng, G. (2021). Near-infrared mitochondria-targetable fluorescent probe for high-contrast bioimaging of H2S. *Anal. Chem.* 93, 5700–5708. doi:10.1021/acs.analchem.0c04639

Goto, N., Hara, H., Kondo, M., Yasuda, N., Kamiya, T., Okuda, K., et al. (2020). Hydrogen sulfide increases copper-dependent neurotoxicity via intracellular copper accumulation. *Metallomics* 12, 868–875. doi:10.1039/D0MT00015A

Greenamyre, J. T. (2018). What's wrong with mitochondria in Parkinson's disease? *Mov. Disord.* 33, 1515–1517. doi:10.1002/mds.98

Greenwood, H. E., and Witney, T. H. (2021). Latest advances in imaging oxidative stress in cancer. *J. Nucl. Med.* 62, 1506–1510. doi:10.2967/jnumed.120.256974

Grunewald, A., Kumar, K. R., and Sue, C. M. (2019). New insights into the complex role of mitochondria in Parkinson's disease. *Prog. Neurobiol.* 177, 73–93. doi:10.1016/j.pneurobio.2018.09.003

Hanaoka, K., Iwaki, S., Yagi, K., Myochin, T., Ikeno, T., Ohno, H., et al. (2022). General design strategy to precisely control the emission of fluorophores via a twisted intramolecular charge transfer (TICT) process. *J. Am. Chem. Soc.* 144, 19778–19790. doi:10.1021/jacs.2c06397

He, W.-M., Zhou, Z., Han, Z., Li, S., Zhou, Z., Ma, L.-F., et al. (2021). Ultrafast size expansion and turn-on luminescence of atomically precise silver clusters by hydrogen sulfide. *Angew. Chem. Int. Ed.* 60, 8505–8509. doi:10.1002/anie.202100006

Hicks, S. W., and Machamer, C. E. (2005). Golgi structure in stress sensing and apoptosis. *BBA Mol. Cell. Res.* 1744, 406–414. doi:10.1016/j.bbamcr.2005.03.002

Hirayama, T., Inden, M., Tsuboi, H., Niwa, M., Uchida, Y., Naka, Y., et al. (2019). A golgi-targeting fluorescent probe for labile Fe(ii) to reveal an abnormal cellular iron distribution induced by dysfunction of VPS35. *Chem. Sci.* 10, 1514–1521. doi:10.1039/C8SC04386H

Hirsch, E., Graybiel, A. M., and Agid, Y. A. (1988). Melanized dopaminergic neurons are differentially susceptible to degeneration in Parkinson's disease. *Nature* 334, 345–348. doi:10.1038/334345a0

Holczer, M., Besze, B., Zámbó, V., Csala, M., Bánhegyi, G., and Kapuy, O. (2018). Epigallocatechin-3-Gallate (EGCG) promotes autophagy-dependent survival via influencing the balance of mTOR-AMPK pathways upon endoplasmic reticulum stress. *Oxid. Med. Cell. Longev.* 2018, 1–15. doi:10.1155/2018/6721530

Hou, J.-T., Wang, B., Zou, Y., Fan, P., Chang, X., Cao, X., et al. (2020a). Molecular fluorescent probes for imaging and evaluation of hypochlorite fluctuations during diagnosis and therapy of osteoarthritis in cells and in a mouse model. *ACS Sens.* 5, 1949–1958. doi:10.1021/acssensors.0c00270

Hou, J.-T., Yu, K.-K., Sunwoo, K., Kim, W. Y., Koo, S., Wang, J., et al. (2020b). Fluorescent imaging of reactive oxygen and nitrogen species associated with pathophysiological processes. *Chem* 6, 832–866. doi:10.1016/j.chempr.2019.12.005

Hou, J.-T., Kwon, N., Wang, S., Wang, B., He, X., Yoon, J., et al. (2022). Sulfur-based fluorescent probes for HOCl: Mechanisms, design, and applications. *Coord. Chem. Rev.* 450, 214232. doi:10.1016/j.ccr.2021.214232

Hu, Y., Shang, Z., Wang, J., Hong, M., Zhang, R., Meng, Q., et al. (2021). A phenothiazine-based turn-on fluorescent probe for the selective detection of hydrogen sulfide in food, live cells and animals. *Analyst* 146, 7528–7536. doi:10.1039/d1an01762d

Jia, T.-T., Li, Y., and Niu, H. (2022). Recent progress in fluorescent probes for diabetes visualization and drug therapy. *Chemosensors* 10, 280. doi:10.3390/chemosensors10070280

Jiang, N., Li, Y., Shu, T., and Wang, J. (2019). Cytokines and inflammation in adipogenesis: An updated review. *Front. Med.* 13, 314–329. doi:10.1007/s11684-018-0625-0

Jiao, X., Xiao, Y., Li, Y., Liang, M., Xie, X., Wang, X., et al. (2018). Evaluating drug-induced liver injury and its remission via discrimination and imaging of HClO and H2S with a two-photon fluorescent probe. *Anal. Chem.* 90, 7510–7516. doi:10.1021/acs.analchem.8b01106

Johansen, D., Ytrehus, K., and Baxter, G. F. (2006). Exogenous hydrogen sulfide (H_2S) protects against regional myocardial ischemia–reperfusion injury- evidence for a role of K ATP channels. *Basic Res. Cardiol.* 101, 53–60. doi:10.1007/s00395-005-0569-9

Jun, T., Xiaopeng, Y., Fangfang, Z., Di, Z., Saijun, M., and Yong, Y. (2020). Visualizing peroxynitrite fuxes and protective eeffect of endogenous hydrogen sulfide during carbonyl stress in endothelial cell. *Sens. Actuators B Chem.* 330, 129283. doi:10.1016/j.snb.2020.129283

Juvekar, V., Park, S. J., Yoon, J., and Kim, H. M. (2021). Recent progress in the two-photon fluorescent probes for metal ions. *Coord. Chem. Rev.* 427, 213574. doi:10.1016/j.ccr.2020.213574

Kamoun, P., Belardinelli, M.-C., Chabli, A., Lallouchi, K., and Chadefaux-Vekemans, B. (2003). Endogenous hydrogen sulfide overproduction in down syndrome. *Am. J. Med. Genet. A* 116A, 310–311. doi:10.1002/ajmg.a.10847

Kasinath, B. S. (2014). Hydrogen sulfide to the rescue in obstructive kidney injury. *Kidney Inter.: Official J. Inter. Soc. Nephrol.* 85 (6), 1255–1258. doi:10.1038/ki.2013.529

Kasinath, B. S., Feliers, D., and Lee, H. J. (2018). Hydrogen sulfide as a regulatory factor in kidney health and disease. *Biochem. Pharmacol.* 149, 29–41. doi:10.1016/j.bcp.2017.12.005

Kawai, K., Fujitsuka, M., and Maruyama, A. (2021). Single-molecule study of redox reaction kinetics by observing fluorescence blinking. *Acc. Chem. Res.* 54, 1001–1010. doi:10.1021/acs.accounts.0c00754

Kimura, H., Nagai, Y., Umemura, K., and Kimura, Y. (2005). Physiological roles of hydrogen sulfide: Synaptic modulation, neuroprotection, and smooth muscle relaxation. *Antioxid. Redox Signal.* 7, 795–803. doi:10.1089/ars.2005.7.795

Kimura, Y., Goto, Y.-I., and Kimura, H. (2009). Hydrogen sulfide increases glutathione production and suppresses oxidative stress in mitochondria. *Antioxid. Redox Signal.* 12, 1–13. doi:10.1089/ars.2008.2282

Kimura, Y., and Kimura, H. (2004). Hydrogen sulfide protects neurons from oxidative stress. *FASEB J.* 18, 1165–1167. doi:10.1096/fj.04-1815fje

Kong, F., Wang, X., Bai, J., Li, X., Yang, C., Li, Y., et al. (2021). A "Double-locked" probe for the detection of hydrogen sulfide in a viscous system. *Chem. Commun.* 57, 6604–6607. doi:10.1039/d1cc01819a

Koning, A. M., Frenay, A.-R. S., Leuvenink, H. G. D., and Van Goor, H. (2015). Hydrogen sulfide in renal physiology, disease and transplantation-the smell of renal protection. *Nitric Oxide* 46, 37–49. doi:10.1016/j.niox.2015.01.005

Kshirsagar, V., Thingore, C., Gursahani, M., Gawali, N., and Juvekar, A. (2021). Hydrogen sulfide ameliorates lipopolysaccharide-induced memory impairment in mice by reducing apoptosis, oxidative, and inflammatory effects. *Neurotox. Res.* 39, 1310–1322. doi:10.1007/s12640-021-00374-6

Kshirsagar, V. V., Thingore, C., and Juvekar, A. (2020). Hydrogen sulfide alleviates lipopolysaccharide-induced memory impairment, neurodegeneration and neuroinflammation in Swiss albino mice. *Alzheimers Dement.* 16, e036835. doi:10.1002/alz.036835

Kushkevych, I., Dordević, D., and Vítězová, M. (2021). Possible synergy effect of hydrogen sulfide and acetate produced by sulfate-reducing bacteria on inflammatory bowel disease development. *J. Adv. Res.* 27, 71–78. doi:10.1016/j.jare.2020.03.007

Lau, L.-H., Lew, J., Borschmann, K., Thijs, V., and Ekinci, E. I. (2019). Prevalence of diabetes and its effects on stroke outcomes: A meta-analysis and literature review. *J. Diabetes Invest.* 10, 780–792. doi:10.1111/jdi.12932

Lei, G., Zhuang, L., and Gan, B. (2022). Targeting ferroptosis as a vulnerability in cancer. *Nat. Rev. Cancer* 22, 381–396. doi:10.1038/s41568-022-00459-0

Li, S. J., Li, Y. F., Liu, H. W., Zhou, D. Y., Jiang, W. L., Ou-Yang, J., et al. (2018). A dual-response fluorescent probe for the detection of viscosity and H2S and its application in studying their cross-talk influence in mitochondria. *Anal. Chem.* 90, 9418–9425. doi:10.1021/acs.analchem.8b02068

Li, H., Mu, J., Sun, J., Xu, S., Liu, W., Xu, F., et al. (2020). Hydrogen sulfide releasing oridonin derivatives induce apoptosis through extrinsic and intrinsic pathways. *Eur. J. Med. Chem.* 187, 111978. doi:10.1016/j.ejmech.2019.111978

Li H, H., Kim, H., Xu, F., Han, J., Yao, Q., Wang, J., et al. (2022). Activity-based NIR fluorescent probes based on the versatile hemicyanine scaffold: Design strategy, biomedical applications, and outlook. *Chem. Soc. Rev.* 51, 1795–1835. doi:10.1039/d1cs00307k

Li, P. P., He, X., Li, Y., Lam, J. W. Y., Kwok, R. T. K., Wang, C. C., et al. (2022). Recent advances in aggregation-induced emission luminogens in photoacoustic imaging. *Eur. J. Nucl. Med. Mol. Imaging* 49, 2560–2583. doi:10.1007/s00259-022-05726-8

Li, S. S., Huo, F., and Yin, C. (2022). NIR fluorescent probe for dual-response viscosity and hydrogen sulfide and its application in Parkinson's disease model. *Dyes Pigments* 197, 109825. doi:10.1016/j.dyepig.2021.109825

Li, Z. Z., Gao, J., Guo, Z., Zhao, H., Liu, L., Wang, M., et al. (2022). Monitoring the fluctuation of H_2S in insulin-resistant HepG2 cells and diabetic mice with a dual-locked NIR fluorescent probe. *Sens. Actuators B Chem.* 353, 131141. doi:10.1016/j.snb.2021.131141

Li, Y., Wang, Y., Lei, X., Guo, K., Ai, Q., Zhang, F., et al. (2023). Development of a responsive probe for colorimetric and fluorescent detection of bisulfite in food and animal serum samples in 100% aqueous solution. *Food Chem.* 407, 135146. doi:10.1016/j.foodchem.2022.135146

Liang, T., Qiang, T., Ren, L., Cheng, F., Wang, B., Li, M., et al. (2022). Near-infrared fluorescent probe for hydrogen sulfide: High-fidelity ferroptosis evaluation *in vivo* during stroke. *Chem. Sci.* 13, 2992–3001. doi:10.1039/d1sc05930k

Liberale, L., Badimon, L., Montecucco, F., Lüscher, T. F., Libby, P., and Camici, G. G. (2022). Inflammation, aging, and cardiovascular disease. *J. Am. Coll. Cardiol.* 79, 837–847. doi:10.1016/j.jacc.2021.12.017

Lim, G. B. (2018). Perivascular inflammation in coronary spasm. *Nat. Rev. Cardiol.* 15, 134–135. doi:10.1038/nrcardio.2018.9

Lim, H. J., Johnny Ong, C.-A., Tan, J. W.-S., and Ching Teo, M. C. (2019). Utility of positron emission tomography/computed tomography (PET/CT) imaging in the evaluation of sarcomas: A systematic review. *Crit. Rev. Oncol. Hemat.* 143, 1–13. doi:10.1016/j.critrevonc.2019.07.002

Lin, Y., Sahoo, B. R., Ozawa, D., Kinoshita, M., Kang, J., Lim, M. H., et al. (2019). Diverse structural conversion and aggregation pathways of alzheimer's amyloid-beta (1-40). *ACS Nano* 13, 8766–8783. doi:10.1021/acsnano.9b01578

Liu, B., and Tang, B. Z. (2020). Aggregation-induced emission: More is different. *Angew. Chem. Int. Ed.* 59, 9788–9789. doi:10.1002/anie.202005345

Liu, Y., Teng, L., Xu, C., Liu, H. W., Xu, S., Guo, H., et al. (2019). A "Double-Locked" and enzyme-activated molecular probe for accurate bioimaging and hepatopathy differentiation. *Chem. Sci.* 10, 10931–10936. doi:10.1039/c9sc03628h

Liu, J., Wang, X., Cheng, Y., Yu, Y., Zhao, M., Huang, J., et al. (2022). Application of a fluorescent H_2S probe based on excited-state intramolecular proton transfer for detecting latent mechanism of H_2S-induced MCF-7 apoptosis. *Future Med. Chem.* 14, 647–663. doi:10.4155/fmc-2021-0309

Lobb, I., Sonke, E., Aboalsamh, G., and Sener, A. (2015). Hydrogen sulphide and the kidney: Important roles in renal physiology and pathogenesis and treatment of kidney injury and disease. *Nitric Oxide* 46, 55–65. doi:10.1016/j.niox.2014.10.004

Lykhmus, O., Mishra, N., Koval, L., Kalashnyk, O., Gergalova, G., Uspenska, K., et al. (2016). Molecular mechanisms regulating LPS-induced inflammation in the brain. *Front. Mol. Neurosci.* 9, 19. doi:10.3389/fnmol.2016.00019

Ma, S., Qiang, J., Li, L., Mo, Y., She, M., Yang, Z., et al. (2019). An efficient biosensor for monitoring alzheimer's disease risk factors: Modulation and disaggregation of the Aβ aggregation process. *J. Mat. Chem. B* 7, 4124–4132. doi:10.1039/C9TB00291J

Mack, M. (2018). Inflammation and fibrosis. *Matrix Biol.* 68-69, 106–121. doi:10.1016/j.matbio.2017.11.010

Majd, M., Saunders, E. F. H., and Engeland, C. G. (2020). Inflammation and the dimensions of depression: A review. *Front. Neuroendocr.* 56, 100800. doi:10.1016/j.yfrne.2019.100800

Manna, P., Gungor, N., Mcvie, R., and Jain, S. K. (2014). Decreased cystathionine-γ-lyase (CSE) activity in livers of type 1 diabetic rats and peripheral blood mononuclear cells (PBMC) of type 1 diabetic patients. *J. Biol. Chem.* 289, 11767–11778. doi:10.1074/jbc.m113.524645

Mantovani, A., Allavena, P., Sica, A., and Balkwill, F. (2008). Cancer-related inflammation. *Nature* 454, 436–444. doi:10.1038/nature07205

Mendes, J. A., Ribeiro, M. C., Reis Filho, G. J. M. V., Rocha, T., Muscará, M. N., Costa, S. K. P., et al. (2019). Hydrogen sulfide inhibits apoptosis and protects the bronchial epithelium in an allergic inflammation mice model. *Int. Immunopharmacol.* 73, 435–441. doi:10.1016/j.intimp.2019.05.041

Milluzzo, A., Maugeri, A., Barchitta, M., Sciacca, L., and Agodi, A. (2021). Epigenetic mechanisms in type 2 diabetes retinopathy: A systematic review. *Int. J. Mol. Sci.* 22, 10502. doi:10.3390/ijms221910502

Morales, I., Guzman-Martinez, L., Cerda-Troncoso, C., Farias, G. A., and Maccioni, R. B. (2014). Neuroinflammation in the pathogenesis of Alzheimer's disease. A rational framework for the search of novel therapeutic approaches. *Front. Cell. Neurosci.* 8, 112. doi:10.3389/fncel.2014.00112

Ngowi, E. E., Afzal, A., Sarfraz, M., Khattak, S., Zaman, S. U., Khan, N. H., et al. (2021). Role of hydrogen sulfide donors in cancer development and progression. *Int. J. Biol. Sci.* 17, 73–88. doi:10.7150/ijbs.47850

O'neill, S. M., Kabir, Z., Mcnamara, G., and Buckley, C. M. (2017). Comorbid depression and risk of lower extremity amputation in people with diabetes: Systematic review and meta-analysis. *BMJ Open Diab. Res. CA* 5, e000366. doi:10.1136/bmjdrc-2016-000366

Oppenheim, R. W., Flavell, R. A., Vinsant, S., Prevette, D., Kuan, C.-Y., and Rakic, P. (2001). Programmed cell death of developing mammalian neurons after genetic deletion of caspases. *J. Neurosci.* 21, 4752–4760. doi:10.1523/JNEUROSCI.21-13-04752.2001

Ou, P., Wang, Y., Hao, C., Peng, Y., and Zhou, L. Y. (2021). Naphthalimide-based a highly selective two-photon fluorescent probe for imaging of hydrogen sulfide in living cells and inflamed tissue of mouse model. *Spectrochim. Acta. A Mol. Biomol. Spectrosc.* 245, 118886. doi:10.1016/j.saa.2020.118886

Pagliassotti, M. J., Kim, P. Y., Estrada, A. L., Stewart, C. M., and Gentile, C. L. (2016). Endoplasmic reticulum stress in obesity and obesity-related disorders: An expanded view. *Metabolism* 65, 1238–1246. doi:10.1016/j.metabol.2016.05.002

Pal, V. K., Bandyopadhyay, P., and Singh, A. (2018). Hydrogen sulfide in physiology and pathogenesis of bacteria and viruses. *IUBMB Life* 70, 393–410. doi:10.1002/iub.1740

Papapetropoulos, A. (2016). Regulation of angiogenesis by hydrogen sulfide. *Free Radic. Bio. Med.* 96, S4. doi:10.1016/j.freeradbiomed.2016.04.035

Park, S. Y., Yoon, S. A., Cha, Y., and Lee, M. H. (2021). Recent advances in fluorescent probes for cellular antioxidants: Detection of NADH, hNQO1, H_2S, and other redox biomolecules. *Coord. Chem. Rev.* 428, 213613. doi:10.1016/j.ccr.2020.213613

Paul, B. D., Sbodio, J. I., Xu, R., Vandiver, M. S., Cha, J. Y., Snowman, A. M., et al. (2014). Cystathionine γ-lyase deficiency mediates neurodegeneration in huntington's disease. *Nature* 509, 96–100. doi:10.1038/nature13136

Poelma, C. (2016). Ultrasound imaging velocimetry: A review. *Exp. Fluids* 58, 3. doi:10.1007/s00348-016-2283-9

Predmore, B. L., Lefer, D. J., and Gojon, G. (2012). Hydrogen sulfide in biochemistry and medicine. *Antioxid. Redox Sign* 17, 119–140. doi:10.1089/ars.2012.4612

Qi, Y.-L., Wang, H.-R., Chen, L.-L., Duan, Y.-T., Yang, S.-Y., and Zhu, H.-L. (2022). Recent advances in small-molecule fluorescent probes for studying ferroptosis. *Chem. Soc. Rev.* 51, 7752–7778. doi:10.1039/D1CS01167G

Qiu, Y., Cao, Y., Cao, W., Jia, Y., and Lu, N. (2020). The application of ferroptosis in diseases. *Pharmacol. Res.* 159, 104919. doi:10.1016/j.phrs.2020.104919

Rajasekar, M. (2021). Recent trends in rhodamine derivatives as fluorescent probes for biomaterial applications. *J. Mol. Struct.* 1235, 130232. doi:10.1016/j.molstruc.2021.130232

Ramya, A. N., Joseph, M. M., Karunakaran, V., Ahammed, C. V. S., Samanta, A., and Maiti, K. K. (2022). An efficient molecular luminophore based on tetraphenylethylene (TPE) enabling intracellular detection and therapeutic benefits of hydrogen sulfide in alzheimer's disease. *Sens. Actuators B Chem.* 355, 131118. doi:10.1016/j.snb.2021.131118

Reddy, P. H. (2009). Role of mitochondria in neurodegenerative diseases: Mitochondria as a therapeutic target in alzheimer's disease. *CNS Spectr.* 14, 8–13. doi:10.1017/S1092852900024901

Ren, M., Xu, Q., Bai, Y., Wang, S., and Kong, F. (2021). Construction of a dual-response fluorescent probe for copper (II) ions and hydrogen sulfide (H_2S) detection in cells and its application in exploring the increased copper-dependent cytotoxicity in present of H_2S. *Spectrochim. Acta. A Mol. Biomol. Spectrosc.* 249, 119299. doi:10.1016/j.saa.2020.119299

Ren, T. B., Wang, Z. Y., Xiang, Z., Lu, P., Lai, H. H., Yuan, L., et al. (2021). A general strategy for development of activatable NIR-II fluorescent probes for *in vivo* high-contrast bioimaging. *Angew. Chem. Int. Ed.* 60, 800–805. doi:10.1002/anie.202009986

Scammahorn, J. J., Nguyen, I. T. N., Bos, E. M., Van Goor, H., and Joles, J. A. (2021). Fighting oxidative stress with sulfur: Hydrogen sulfide in the renal and cardiovascular systems. *Antioxidants* 10, 373. doi:10.3390/antiox10030373

Sedgwick, A. C., Dou, W. T., Jiao, J. B., Wu, L., Williams, G. T., Jenkins, A., et al. (2018). An ESIPT probe for the ratiometric imaging of peroxynitrite facilitated by binding to aβ-aggregates. *J. Am. Chem. Soc.* 140, 14267–14271. doi:10.1021/jacs.8b08457

Sempere-Bigorra, M., Julian-Rochina, I., and Cauli, O. (2021). Differences and similarities in neuropathy in type 1 and 2 diabetes: A systematic review. *J. Pers. Med.* 11, 230. doi:10.3390/jpm11030230

Shen, W., Wang, P., Xie, Z., Zhou, H., Hu, Y., Fu, M., et al. (2021). A bifunctional probe reveals increased viscosity and hydrogen sulfide in zebra fish model of Parkinson's disease. *Talanta* 234, 122621. doi:10.1016/j.talanta.2021.122621

Shu, W., Zang, S., Wang, C., Gao, M., Jing, J., and Zhang, X. (2020). An endoplasmic reticulum-targeted ratiometric fluorescent probe for the sensing of hydrogen sulfide in living cells and zebrafish. *Anal. Chem.* 92, 9982–9988. doi:10.1021/acs.analchem.0c01623

Sica, A., Wang, J. M., Colotta, F., Dejana, E., Matsushima, K., Oppenheim, J. J., et al. (1990). Monocyte chemotactic and activating factor gene expression induced in endothelial cells by IL-1 and tumor necrosis factor. *J. Immunol.* 144, 3034–3038. doi:10.4049/jimmunol.144.8.3034

Sies, H. (1997). Oxidative stress: Oxidants and antioxidants. *Exp. Physiol.* 82, 291–295. doi:10.1113/expphysiol.1997.sp004024

Singh, N., Sharma, S., Singh, R., Rajput, S., Chattopadhyay, N., Tewari, D., et al. (2021). A naphthalimide-based peptide conjugate for concurrent imaging and apoptosis induction in cancer cells by utilizing endogenous hydrogen sulfide. *Chem. Sci.* 12, 16085–16091. doi:10.1039/d1sc04030h

Starling, S. (2018). Alzheimer disease: Blood-derived Abeta induces AD pathology. *Nat. Rev. Neurol.* 14, 2. doi:10.1038/nrneurol.2017.164

Su, W., Huang, L., Zhu, L., and Lin, W. (2022). A novel fluorescent probe for imagining hydrogen sulfide upregulation in acute lung injury. *Sens. Actuators B Chem.* 369, 132297. doi:10.1016/j.snb.2022.132297

Sun, H.-J., Wu, Z.-Y., Nie, X.-W., Wang, X.-Y., and Bian, J.-S. (2021). An updated insight into molecular mechanism of hydrogen sulfide in cardiomyopathy and myocardial ischemia/reperfusion injury under diabetes. *Front. Pharmacol.* 12, 651884. doi:10.3389/fphar.2021.651884

Sun, Y., Sun, P., Li, Z., Qu, L., and Guo, W. (2022). Natural flavylium-inspired far-red to NIR-II dyes and their applications as fluorescent probes for biomedical sensing. *Chem. Soc. Rev.* 51, 7170–7205. doi:10.1039/D2CS00179A

Swerdlow, R. H. (2018). Mitochondria and mitochondrial cascades in alzheimer's disease. *J. Alzheimer's Dis.* 62, 1403–1416. doi:10.3233/JAD-170585

Szabo, C., Coletta, C., Chao, C., Módis, K., Szczesny, B., Papapetropoulos, A., et al. (2013). Tumor-derived hydrogen sulfide, produced by cystathionine-β-synthase, stimulates bioenergetics, cell proliferation, and angiogenesis in colon cancer. *Proc. Natl. Acad. Sci. U.S.A.* 110, 12474–12479. doi:10.1073/pnas.1306241110

Tabassum, R., Jeong, N. Y., and Jung, J. (2020). Therapeutic importance of hydrogen sulfide in age-associated neurodegenerative diseases. *Neural Regen. Res.* 15, 653–662. doi:10.4103/1673-5374.266911

Tan, G., Pan, S., Li, J., Dong, X., Kang, K., Zhao, M., et al. (2011). Hydrogen sulfide attenuates carbon tetrachloride-induced hepatotoxicity, liver cirrhosis and portal hypertension in rats. *PLoS One* 6, e25943. doi:10.1371/journal.pone.0025943

Tang, J., Yang, X., Zhao, F., Zhang, D., Mo, S., and Ye, Y. (2021). Visualizing peroxynitrite fluxes and protective effect of endogenous hydrogen sulfide during carbonyl stress in endothelial cell. *Sensors and Actuators B: Chemical* 330, 129283. doi:10.1016/j.snb.2020.129283

Vandini, E., Ottani, A., Zaffe, D., Calevro, A., Canalini, F., Cavallini, G. M., et al. (2019). Mechanisms of hydrogen sulfide against the progression of severe alzheimer's disease in transgenic mice at different ages. *Pharmacology* 103, 50–60. doi:10.1159/000494113

Wallace, J. L. (2007). Hydrogen sulfide-releasing anti-inflammatory drugs. *Trends Pharmacol. Sci.* 28, 501–505. doi:10.1016/j.tips.2007.09.003

Wang, J., and Chen, G.-J. (2016). Mitochondria as a therapeutic target in alzheimer's disease. *Genes Dis.* 3, 220–227. doi:10.1016/j.gendis.2016.05.001

Wang, X.-Y., Yang, C.-T., Zheng, D.-D., Mo, L.-Q., Lan, A.-P., Yang, Z.-L., et al. (2012). Hydrogen sulfide protects H9c2 cells against doxorubicin-induced cardiotoxicity through inhibition of endoplasmic reticulum stress. *Mol. Cell. Biochem.* 363, 419–426. doi:10.1007/s11010-011-1194-6

Wang, R., Lai, X., Qiu, G., and Liu, J. (2019). Recent advances in reaction-based excited state intramolecular proton transfer (ESIPT) fluorescence probe. *Chin. J. Org. Chem.* 39, 952–960. doi:10.6023/cjoc201811006

Wang, H., Li, X., Zhu, Z., Wang, H., Wei, B., and Bai, X. (2020). Hydrogen sulfide promotes lipopolysaccharide-induced apoptosis of osteoblasts by inhibiting the AKT/NF-κB signaling pathway. *Biochem. Biophys. Res. Commun.* 524, 832–838. doi:10.1016/j.bbrc.2020.02.005

Wang, K., Yang, X., Guo, M.-Y., Chen, X.-Y., Li, T., Yan, R., et al. (2022). Imaging the dynamic processes of hydrogen sulfide using a rapid "turn-on" mitochondria-targeting fluorescent probe. *Sens. Actuators B Chem.* 369, 132285. doi:10.1016/j.snb.2022.132285

Wang, W. X., Wang, Z. Q., Tan, Z. K., Mao, G. J., Chen, D. H., and Li, C. Y. (2022). A nitrobenzoxadiazole-based near-infrared fluorescent probe for the specific imaging of H_2S in inflammatory and tumor mice. *Analyst* 147, 2712–2717. doi:10.1039/d2an00623e

Wang, Y., Li, S., Zhu, X., Shi, X., Liu, X., and Zhang, H. (2022). A novel H_2O_2 activated NIR fluorescent probe for accurately visualizing H_2S fluctuation during oxidative stress. *Anal. Chim. Acta* 1202, 339670. doi:10.1016/j.aca.2022.339670

Wei, W., Wang, C., Li, D., and Yang, Z. (2017). The content of hydrogen sulfide in plasma of cirrhosis rats combined with portal hypertension and the correlation with indexes of liver function and liver fibrosis. *Exp. Ther. Med.* 14, 5022–5026. doi:10.3892/etm.2017.5133

Weiss, G., Ganz, T., and Goodnough, L. T. (2019). Anemia of inflammation. *Blood* 133, 40–50. doi:10.1182/blood-2018-06-856500

Whiteman, M., Gooding, K. M., Whatmore, J. L., Ball, C. I., Mawson, D., Skinner, K., et al. (2010). Adiposity is a major determinant of plasma levels of the novel vasodilator hydrogen sulphide. *Diabetol* 53, 1722–1726. doi:10.1007/s00125-010-1761-5

Wlodkowic, D., Skommer, J., Mcguinness, D., Hillier, C., and Darzynkiewicz, Z. (2009). ER-golgi network-A future target for anti-cancer therapy. *Leuk. Res.* 33, 1440–1447. doi:10.1016/j.leukres.2009.05.025

Wood, H. (2017). Alzheimer disease:peripheral Aβ clearance - a therapeutic strategy for AD? *Nat. Rev. Neurol.* 13, 386. doi:10.1038/nrneurol.2017.80

Wu, D., Gu, Y., and Zhu, D. (2021). Cardioprotective effects of hydrogen sulfide in attenuating myocardial ischemia-reperfusion injury (review). *Mol. Med. Rep.* 24, 875. doi:10.3892/mmr.2021.12515

Wu, W., and Liu, B. (2021). Aggregation-induced emission: Challenges and opportunities. *Natl. Sci. Rev.* 8, nwaa222. doi:10.1093/nsr/nwaa222

Xiang, A. H., Wang, X., Martinez, M. P., Getahun, D., Page, K. A., Buchanan, T. A., et al. (2018). Maternal gestational diabetes mellitus, type 1 diabetes, and type 2 diabetes during pregnancy and risk of ADHD in offspring. *Diabetes Care* 41, 2502–2508. doi:10.2337/dc18-0733

Xing, P., Gao, K., Wang, B., Gao, J., Yan, H., Wen, J., et al. (2016). HEPES is not suitable for fluorescence detection of HClO: A novel probe for HClO in absolute PBS. *Chem. Commun.* 52, 5064–5066. doi:10.1039/c6cc00880a

Xu, L., Zhang, J., Yin, L., Long, X., Zhang, W., and Zhang, Q. (2020). Recent progress in efficient organic two-photon dyes for fluorescence imaging and photodynamic therapy. *J. Mat. Chem. C* 8, 6342–6349. doi:10.1039/D0TC00563K

Yang, L., Zhang, Y., Ren, X., Wang, B., Yang, Z., Song, X., et al. (2020). Fluorescent detection of dynamic H2O2/H2S redox event in living cells and organisms. *Anal. Chem.* 92, 4387–4394. doi:10.1021/acs.analchem.9b05270

Yin, W.-L., Yin, W.-G., Huang, B.-S., and Wu, L.-X. (2017). Neuroprotective effects of lentivirus-mediated cystathionine-beta-synthase overexpression against 6-OHDA-induced Parkinson's disease rats. *Neurosci. Lett.* 657, 45–52. doi:10.1016/j.neulet.2017.07.019

Ying, R., Wang, X.-Q., Yang, Y., Gu, Z.-J., Mai, J.-T., Qiu, Q., et al. (2016). Hydrogen sulfide suppresses endoplasmic reticulum stress-induced endothelial-to-mesenchymal transition through src pathway. *Life Sci.* 144, 208–217. doi:10.1016/j.lfs.2015.11.025

Yu, S., Jia, J., Zheng, J., Zhou, Y., Jia, D., and Wang, J. (2021). Recent progress of ferroptosis in lung diseases. *Front. Cell. Dev. Biol.* 9, 789517. doi:10.3389/fcell.2021.789517

Zhang, M., Shan, H., Wang, T., Liu, W., Wang, Y., Wang, L., et al. (2013). Dynamic change of hydrogen sulfide after traumatic brain injury and its effect in mice. *Neurochem. Res.* 38, 714–725. doi:10.1007/s11064-013-0969-4

Zhang, C., Zhang, Q. Z., Zhang, K., Li, L. Y., Pluth, M. D., Yi, L., et al. (2019). Dual-biomarker-triggered fluorescence probes for differentiating cancer cells and revealing synergistic antioxidant effects under oxidative stress. *Chem. Sci.* 10, 1945–1952. doi:10.1039/c8sc03781g

Zhang, Y., Masters, L., Wang, Y., Wu, L., Pei, Y., Guo, B., et al. (2021). Cystathionine gamma-lyase/H_2S signaling facilitates myogenesis under aging and injury condition. *FASEB J.* 35, e21511. doi:10.1096/fj.202002675r

Zhao, W. K., Zhou, Y., Xu, T. T., and Wu, Q. (2021). Ferroptosis: Opportunities and challenges in myocardial ischemia-reperfusion injury. *Oxidative Med. Cell. Longev.* 2021, 1–12. doi:10.1155/2021/9929687

Zhao, L., Zhou, X., Xie, F., Zhang, L., Yan, H., Huang, J., et al. (2022). Ferroptosis in cancer and cancer immunotherapy. *Cancer Commun.* 42, 88–116. doi:10.1002/cac2.12250

Zhao, Y., Shi, W., Li, X., and Ma, H. (2022). Recent advances in fluorescent probes for lipid droplets. *Chem. Commun.* 58, 1495–1509. doi:10.1039/D1CC05717K

Zhu, H., Liang, C., Cai, X., Zhang, H., Liu, C., Jia, P., et al. (2020a). Rational design of a targetable fluorescent probe for visualizing H2S production under Golgi stress response elicited by monensin. *Anal. Chem.* 92, 1883–1889. doi:10.1021/acs.analchem.9b04009

Zhu, H., Liu, C., Liang, C., Tian, B., Zhang, H., Zhang, X., et al. (2020b). A new phenylsulfonamide-based golgi-targeting fluorescent probe for H_2S and its bioimaging applications in living cells and zebrafish. *Chem. Commun.* 56, 4086–4089. doi:10.1039/d0cc00282h

Zimmermann, K. K., Spassov, S. G., Strosing, K. M., Ihle, P. M., Engelstaedter, H., Hoetzel, A., et al. (2018). Hydrogen sulfide exerts anti-oxidative and anti-inflammatory effects in acute lung injury. *Inflammation* 41, 249–259. doi:10.1007/s10753-017-0684-4